

Numerical solution of a nonlinear Fredholm integral equation of the first kind
by Katarzyna Kuglarz Jonca

A thesis submitted in partial fulfillment of the requirements for the degree of Doctor of Philosophy in Mathematics
Montana State University
© Copyright by Katarzyna Kuglarz Jonca (1988)

Abstract:
A numerical method for nonlinear Fredholm first kind integral equations is presented. These equations are ill-posed, ie., small perturbations in the data may give rise to large perturbations in the solution. To obtain stable, accurate solutions, the method of Tikhonov Regularization is used. We develop a quasi-Newton/trust region algorithm to solve the unconstrained minimization problem which arises when regularization is used. This algorithm is applied to an ill-posed inverse problem arising in geophysics. We present results of a numerical study of the effects of discretization, error in the data, choice of the regularization parameter, and parameters in the physical model on the stability and accuracy of the approximate solutions.

NUMERICAL SOLUTION OF A NONLINEAR FREDHOLM INTEGRAL EQUATION OF THE FIRST KIND

by

Katarzyna Kuglarz Jonca

A thesis submitted in partial fulfillment
of the requirements for the degree

of

Doctor of Philosophy

in

Mathematics

MONTANA STATE UNIVERSITY
Bozeman, Montana

March, 1988

D378
J6981

APPROVAL

of a thesis submitted by

Katarzyna Kuglarz Jonca

This thesis has been read by each member of the thesis committee and has been found to be satisfactory regarding content, English usage, format, citations, bibliographic style, and consistency, and is ready for submission to the College of Graduate Studies.

Feb 29, 1988
Date

Curtis R. Vogel
Chairperson,
Graduate Committee

Approved for the Major Department

2/29/88
Date

Head, Major Department

Approved for the College of Graduate Studies

3-4-88
Date

Graduate Dean

STATEMENT OF PERMISSION TO USE

In presenting this thesis in partial fulfillment of the requirements for a doctoral degree at Montana State University, I agree that the Library shall make it available to borrowers under rules of the Library. I further agree that copying of this thesis is allowable only for scholarly purposes, consistent with "fair use" as prescribed in the U.S. Copyright Law. Requests for extensive copying or reproduction of this thesis should be referred to University Microfilms International, 300 North Zeeb Road, Ann Arbor, Michigan 48106, to whom I have granted "the exclusive right to reproduce and distribute copies of the dissertation in and from microfilm and the right to reproduce and distribute by abstract in any format."

Signature Katarzyna Jonca

Date 02/29/88

ACKNOWLEDGMENTS

I would like to thank Professor Curtis Vogel for his constant support, encouragement and all his helpful discussions with me during my work on this thesis.

I also want to thank Professor Gary Bogar for moral support and words of optimism given so often to me.

Finally, I would like to thank Professors John Lund and Ken Bowers for their helpful suggestions.

TABLE OF CONTENTS

	Page
1. INTRODUCTION	1
2. THEORETICAL BACKGROUND	4
Hilbert Spaces	4
Weak Convergence and Weak Continuity	5
Compactness, Weak Compactness and Compact Operators	7
Frechet Derivative	9
Compact Self-Adjoint Linear Operators	10
Singular Value Decomposition	11
Moore-Penrose Generalized Inverse	13
Ill-Posedness	14
Tikhonov Regularization	16
Tikhonov Regularization in the Linear Case	19
Linearization of a Nonlinear Problem	20
Choice of the Regularization Parameter	22
3. THE MAGNETIC RELIEF PROBLEM	24
Derivation of the System	24
Ill-Posedness of the Problem	30
4. NUMERICAL OPTIMIZATION	32
1-D Case	32
2-D Case	34
Globally Convergent Minimization Algorithm	38
5. NUMERICAL RESULTS FOR MAGNETIC RELIEF PROBLEM	46
Linearized Stability Analysis	46
Computational Results	50
REFERENCES CITED	57

LIST OF FIGURES

Figure		Page
1.	Geometry of the Magnetic Relief Problem	25
2.	Definition of the Vectors **r** and **p**	26
3.	Derivative Kernel $\frac{\partial k_x}{\partial f'}$ for $h = 0.1$ and $h = 0.2$	47
4.	Derivative Kernel $\frac{\partial k_x}{\partial f}$ for $h = 0.1$ and $h = 0.2$	48
5.	Singular Values of the Derivative	49
6.	Approximate Solutions for $h = 0.1$	51
7.	Approximate Solutions for $h = 0.2$	52
8.	$\|e(\alpha)\|$ and $V(\alpha)$ vs α (1-D Case)	53
9.	Approximate Solutions	54
10.	Approximate Solutions on Diagonal $x = y$	55
11.	$\|e(\alpha)\|$ and $V(\alpha)$ vs α (2-D Case)	56

ABSTRACT

A numerical method for nonlinear Fredholm first kind integral equations is presented. These equations are ill-posed, i.e., small perturbations in the data may give rise to large perturbations in the solution. To obtain stable, accurate solutions, the method of Tikhonov Regularization is used. We develop a quasi-Newton/trust region algorithm to solve the unconstrained minimization problem which arises when regularization is used. This algorithm is applied to an ill-posed inverse problem arising in geophysics. We present results of a numerical study of the effects of discretization, error in the data, choice of the regularization parameter, and parameters in the physical model on the stability and accuracy of the approximate solutions.

CHAPTER 1

INTRODUCTION

In this thesis we consider the numerical solution of a nonlinear ill-posed Hilbert space operator equation

$$K(f) = g \tag{1.1}$$

which arises in geophysics. One wants to determine the shape of the boundary between the magnetized rock and unmagnetized sediments which cover it, from the air-borne measurements of the magnetic field [1]. The mathematical model describing this problem consists of a system of nonlinear Fredholm integral equations of the first kind. Similar problems are frequently encountered in other applications. Examples include geophysics [1], [21], inverse scattering [2], remote sensing of the atmosphere [12], [29] and biology [20] to mention only a few.

The ill-posedness of the problem means that small perturbations in the data g on the right hand side of (1.1) may cause big changes in the solution f. This is manifested in the frequently observed fact that simple discretization or collocation methods do not give satisfactory approximate solutions to (1.1). Any consistent discretization of the system will be ill-conditioned and, as $n \to \infty$, any norm of the approximate solution typically becomes unbounded. This phenomenon is especially pronounced when the data g is error contaminated. Thus to numerically solve problem (1.1) special methods are required. They are called regularization methods. In this thesis, we apply the Tikhonov regularization method [3], [4], [5] to the problem (1.1).

In the Tikhonov regularization method the problem (1.1) is replaced by the minimization problem

$$\min_f \{\|K(f) - g\|^2 + \alpha J(f)\}, \tag{1.2}$$

where α is a positive, parameter called the regularization or smoothing parameter, and J is a penalty functional. Different penalty functionals can be used [4], [14]. In this thesis the penalty term is

$$J(f) = \|f\|^2$$

where $\|\cdot\|$ is an appropriate Hilbert space norm.

Tikhonov regularization is probably the most popular regularization method currently used for nonlinear ill-posed problems. Other regularization methods which are frequently discussed in the literature include the method of quasi-solutions [3], [4], and, for linear problems, the truncated singular value decomposition method, which is often called the method of spectral cut-off [6], [7], [8], [9], and the Landweber-Fridman iterative method [10], [11], [5].

An important and difficult practical problem is the choice of the regularization parameter α. If α is too large the approximate solution does not correspond to the data g; if α is too small, the norm of the approximate solution will be unduly large. There are a number of studies concerned with the choice of the parameter α [22], [23], [24]. In this thesis we use the Generalized Cross Validation (GCV) method [13] to choose α.

To numerically solve the regularized problem (1.2) we first discretize it. A quasi-Newton iterative method with the trust region approach [15] is then used. In this way global convergence is achieved, and the fast convergence of the quasi-Newton method is retained close to the solution. At each iteration the resulting

system of equations is diagonalized using the Singular Value Decomposition. This ensures numerical stability, allows easy computation of the GCV estimate for the optimal value of the regularization parameter, and gives a characterization of the degree of ill-posedness of the problem.

The thesis is organized as follows: Chapter 2 contains some background theory for compact operators, and in particular, integral operators of the first kind. Necessary ideas such as weak compactness, weak continuity, ill-posedness, and regularization are reviewed. Chapter 3 describes in detail the geophysical inverse problem considered in the thesis. A derivation of the system of nonlinear integral equations of the first kind for this problem is given. Then a stable and efficient numerical method for solving the regularized problem is presented in Chapter 4. Chapter 5 gives a linearized stability analysis for the geophysical inverse problem and numerical results. Both a simplified one-dimensional (1-D) version of the problem and the more complicated two-dimensional (2-D) case are presented.

CHAPTER 2

THEORETICAL BACKGROUND

Hilbert Spaces

Let X be a Hilbert space with inner product denoted by

$$\langle u, v\rangle, \quad u, v \in X,$$

and induced norm

$$\|u\| = \sqrt{\langle u, u\rangle}, \quad u \in X.$$

Example 2.1: We introduce important Hilbert spaces used in this thesis

(i) $L^2(\Omega)$ is the set of all equivalence classes of functions $f : \Omega \to R$, $\Omega \subset R^n$, such that $\int_\Omega f^2(x)\,dx$ exists and is finite. The inner product is defined as

$$\langle f, g\rangle := \int_\Omega f(x)g(x)\,dx.$$

(ii) The Sobolev space $H^1(\Omega)$ (see [25], [26]) is the set of all functions $f : \Omega \to R$ such that $\frac{\partial f}{\partial x_i} \in L^2(\Omega)$, $i = 1, 2, ..., n$. The standard inner product is defined as

$$\langle f, g\rangle := \int_\Omega fg\,dx + \int_\Omega \nabla f \cdot \nabla g\,dx. \tag{2.2}$$

An inner product yielding a norm equivalent to the norm induced by (2.2) is

$$\langle f, g\rangle = \int_{\partial\Omega} fg\,ds + \int_\Omega \nabla f \cdot \nabla g\,dx.$$

The subspace of functions from $H^1(\Omega)$ vanishing on the boundary will be denoted by $H_0^1(\Omega)$. On this subspace we will use the inner product

$$\langle f, g \rangle = \int_\Omega \nabla f \cdot \nabla g \, dx. \tag{2.3}$$

Definition 2.4: If $A : X \to Y$, where X, Y are Hilbert spaces, is a bounded linear operator, then $A^* : Y \to X$ is called the adjoint operator of A if for all $x \in X$ and $y \in Y$,

$$\langle Ax, y \rangle = \langle x, A^* y \rangle.$$

Weak Convergence and Weak Continuity

Definition 2.5: The set of all continuous linear functionals on X, that is, the set of all $x^* : X \to R$ such that x^* is linear and continuous, is called the dual of X and is denoted by X^*.

In a Hilbert space X, the dual space X^* is isometrically isomorphic to X.

Definition 2.6: We say that a sequence $\{x_n\} \subset X$ converges to x if

$$\forall \epsilon > 0 \quad \exists N \quad \forall n \geq N \quad \|x_n - x\| \leq \epsilon.$$

This convergence is also called norm, or strong, convergence, and is denoted by $x_n \to x$.

Definition 2.7: We say that a sequence $\{x_n\} \subset X$ converges weakly to x and write $x_n \rightharpoonup x$ if

$$\forall x^* \in X^* \quad x^*(x_n) \to x^*(x).$$

In case of $dim X < \infty$, weak convergence coincides with (strong or norm) convergence. However in an infinite dimensional vector space a sequence may converge weakly but fail to converge.

Example 2.8: Consider any orthonormal sequence $\{e_n\} \subset X$, where X is a Hilbert space. We show that $e_n \rightharpoonup 0$ but does not converge strongly. We have

$$\forall x \in X \qquad \sum_{j=1}^{\infty} |\langle x, e_j \rangle|^2 \leq \|x\|^2 \qquad \text{(Bessel's inequality)}$$

so $\lim_{j \to \infty} \langle x, e_j \rangle = 0$ is a necessary condition for convergence of the series. From the Riesz Theorem [16], $x^*(e_j) = \langle e_j, x \rangle$ so $\forall x^* \in X^* \quad x^*(e_j) = \langle e_j, x \rangle \to 0 = x^*(0)$. On the other hand $\{e_n\}$ is not a Cauchy sequence because

$$\forall n, m \quad \|e_n - e_m\|^2 = \langle e_n - e_m, e_n - e_m \rangle = \|e_n\|^2 + \|e_m\|^2 = 2.$$

Thus the sequence is not convergent.

Definition 2.9: $F : X \to Y$ is weakly continuous if

$$\forall x_n \rightharpoonup x \quad F(x_n) \to F(x).$$

Example 2.10: Let $X = H_0^1(\Omega)$, $Y = L^2(\Omega)$, $\Omega = (0,1)$, $K : X \to Y$, and

$$[K(x)](s) := \int_0^1 k(s, t, x(t))\, dt$$

where $k : \Omega \times \Omega \times R \to R$ has a continuous partial derivative with respect to the third argument. Then K is a weakly continuous operator.

Proof: Let $x_n \rightharpoonup x$. We need to show that $K(x_n) \to K(x)$ in L^2 norm. For

every $s \in \Omega$, we have

$$\begin{aligned}|[K(x_n)](s) - [K(x)](s)| &\leq \int_0^1 |k(s,t,x_n(t)) - k(s,t,x(t))|\, dt \\ &= \int_0^1 |\frac{\partial k}{\partial x}(s,t,\xi_n(t))||x_n(t) - x(t)|\, dt \\ &\leq C \int_0^1 |x_n(t) - x(t)|\, dt \\ &\leq C \sup_{t\in[0,1]} |x_n(t) - x(t)|.\end{aligned}$$

However, weak convergence in $H_0^1(\Omega)$ implies uniform convergence. Therefore we see that $K(x_n)$ converges uniformly to $K(x)$. Since the uniform norm is stronger than the L^2 norm the proof is complete.

Compactness, Weak Compactness and Compact Operators

Definition 2.11: Let X be a normed space. A set $M \subset X$ is called compact if every sequence $\{x_n\} \subset M$ has a subsequence converging to an element $x \in M$. A set M is called relatively compact if its closure $\overline{M}$ is compact.

Definition 2.12: Let X be a normed space. A set $M \subset X$ is called weakly compact if every sequence $\{x_n\} \subset M$ has a subsequence weakly converging to an element $x \in M$. A set M is called weakly relatively compact if its closure $\overline{M}$ is weakly compact.

Theorem 2.13: Let X be a Hilbert space. Then M is bounded if and only if M is weakly relatively compact.

Proof: See [18].

Definition 2.14: Let X and Y be Hilbert spaces. An operator $A : X \to Y$ is called a compact operator if A is continuous, and for every bounded subset M of X, the image $A(M)$ is relatively compact.

Theorem 2.15: If K is a weakly continuous operator, then K is compact.

Proof: Let $\{x_n\} \subset X$ be bounded. We need to show that $\{K(x_n)\}$ has a convergent subsequence. By Theorem 2.13 every bounded sequence possesses a weakly convergent subsequence. Let us denote it by $\{x_{n_j}\}$:

$$\exists x_0 \in X \quad x_{n_j} \rightharpoonup x_0.$$

Since K is weakly continuous, $K(x_{n_j}) \to K(x_0)$. Also, if K is weakly continuous, it is continuous because taking $x_n \to x$ we obtain $x_n \rightharpoonup x$ and hence $K(x_n) \to K(x)$.

Example 2.16: We give the following examples of linear and nonlinear compact integral operators

(i) Let $K : X \to Y$ where $X = L^2(\Omega)$, $Y = L^2(\Omega)$, $\Omega = (0,1)$, and define

$$(Kx)(s) = \int_0^1 k(s,t)x(t)\,dt$$

where k is any square integrable function, that is, k^2 is integrable over $\Omega \times \Omega$. Then K is a linear compact operator. For a proof see [27].

(ii) Let $K : X \to Y$ where $X = H^1(\Omega)$, $Y = L^2(\Omega)$, $K : X \to Y$, and define

$$[K(x)](s) = \int_\Omega k(s,t,x(t))\,dt,$$

where $\dfrac{\partial k}{\partial x}$ is continuous. By Example 2.10 and Theorem 2.15 K is a compact operator.

Frechet Derivative

Definition 2.17: Let $A : X \to Y$ be an arbitrary operator, and let X and Y be Banach spaces. We say that A is differentiable at x_0 if there exists a continuous linear mapping $A'(x_0) : X \to Y$ such that

$$A(x_0 + h) - A(x_0) = A'(x_0)h + r(h)$$

where $\lim_{h \to 0} \frac{\|r(h)\|}{\|h\|} = 0$. $A'(x_0)$ is called a strong or Frechet derivative of A at the point x_0.

The derivative of a continuous linear operator as well as the derivative of the Hilbert space norm will be used frequently in the sequel. We derive them in the following examples.

Example 2.18: Let $A : X \to Y$ be a linear bounded operator. Then

$$A(x_0 + h) - Ax_0 = Ah.$$

Therefore $r(h) = 0$ and $A'(x_0) = A$.

Example 2.19: Let $T : X \to R$ where X is a Hilbert space and $T(x) := \|x\|^2$. We have

$$\|x_0 + h\|^2 - \|x_0\|^2 = \|x_0\|^2 + 2\langle x_0, h\rangle + \|h\|^2 - \|x_0\|^2 = 2\langle x, h\rangle + \|h\|^2.$$

Therefore $r(h) = \|h\|^2$ and $\lim_{h \to 0} \frac{\|r(h)\|}{\|h\|} = 0$. We get $T'(x_0)h = \langle 2x_0, h\rangle$, so $T'(x_0) = 2x_0$.

Compact Self-Adjoint Linear Operators

Definition 2.20: Let $B : X \to X$ be a bounded linear operator on a Hilbert space X. B is called a self-adjoint operator if $B^* = B$.

Theorem 2.21 (Spectral Theorem for Compact Self-Adjoint Linear Operators): Let $B : X \to X$ be a self-adjoint compact linear operator. Then

$$Bx = \sum_{i \in I} \lambda_i \langle x, v_i \rangle v_i$$

where the $\lambda_i's$ are eigenvalues of B, the $v_i's$ are corresponding orthonormal eigenvectors, and I is an index set for the eigenvalues. Since B is compact, I is a countable set (possibly finite). If I is infinite, 0 is a limit point of the spectrum of B. Each λ_i is repeated in the sum according to its multiplicity.

Proof: See [17].

We denote by $\sigma(B)$ the spectrum of a linear operator B.

Theorem 2.22: If B is a compact linear self-adjoint operator and $f : \sigma(B) \to R$ is continuous, then $\sigma(f(B)) = f(\sigma(B))$.

Proof: See [18].

Example 2.23: Given a compact linear self-adjoint operator $B : X \to X$ and its spectrum $\sigma(B)$, we can find the spectrum of the operator $B + \alpha I$ by applying Theorem 2.22. We have

$$\sigma(B + \alpha I) = \sigma(B) + \alpha.$$

Singular Value Decomposition

Let $A : X \to Y$ (X, Y Hilbert spaces) be a compact linear operator. We denote by v_j the orthonormal eigenvectors of A^*A

$$A^*Av_j = \lambda_j v_j.$$

All eigenvalues λ_j are nonnegative because

$$\lambda_j = \lambda_j \langle v_j, v_j \rangle = \langle A^*Av_j, v_j \rangle = \langle Av_j, Av_j \rangle \geq 0. \tag{2.24}$$

Therefore one can introduce the singular values σ_j of the operator A: For $\lambda_j > 0$,

$$\sigma_j = \sqrt{\lambda_j}. \tag{2.25}$$

Now define $u_j := \dfrac{1}{\sigma_j} Av_j$. One can show easily that

$$AA^*u_j = \lambda_j u_j, \qquad \langle u_j, u_k \rangle = \delta_{jk},$$

$$Av_j = \sigma_j u_j, \qquad \text{and} \qquad A^*u_j = \sigma_j v_j.$$

The triple $\{u_i; \sigma_i; v_i\}$ is called a singular system for A.

To discuss the representation of A in terms of singular values we need to introduce the following:

Definition 2.26: Let $A : X \to Y$. The image of X under A (range of A) will be denoted by $\mathcal{R}(A)$. In other words

$$\mathcal{R}(A) := \{y \in Y : \ \exists x \in X \quad A(x) = y\}.$$

Also the kernel (null space) of A is the inverse image of $0 \in Y$ under A, that is,

$$\mathcal{N}(A) := \{x \in X : \ A(x) = 0\}.$$

It can be shown using the Spectral Theorem 2.21 that the set $\{u_i\}$ is a complete orthonormal set for $\overline{\mathcal{R}(A)}$ and the set $\{v_i\}$ is a complete orthonormal set for the orthogonal complement of $\mathcal{N}(A)$, denoted by $\mathcal{N}(A)^\perp$. Using this we can represent any $x \in X$ as $x = x_0 + x_1$, where $x_0 \in \mathcal{N}(A), x_1 \in \mathcal{N}(A)^\perp$ and

$$x_1 = \sum_{i \in I} \langle x_1, v_i \rangle v_i = \sum_{i \in I} \langle x, v_i \rangle v_i .$$

The last equality follows from the fact that $x_0 \in \mathcal{N}(A)$ and hence it is orthogonal to all v_i. We now get a representation for Ax:

$$\begin{aligned} Ax &= A(\sum_{i \in I} \langle x, v_i \rangle v_i + x_0) \\ &= \sum_{i \in I} \langle x, v_i \rangle Av_i \\ &= \sum_{i \in I} \sigma_i \langle x, v_i \rangle u_i . \end{aligned}$$

Definition 2.27 (Singular Value Decomposition of a Matrix): If $dim X = n$ and $dim Y = m$ then the singular system of A consisting of the vectors u_i, v_i and singular values σ_i may be described in the following way. Vectors v_i can be treated as n columns of an $n \times n$ matrix V. Vectors u_i make up an $m \times m$ matrix U. Both matrices are orthogonal. The singular values σ_i lie on the main diagonal of an $m \times n$ matrix D, which in the case of $m \geq n$ means

$$[D]_{ij} = \begin{cases} \sigma_i, & \text{if } i = j \leq n; \\ 0, & \text{otherwise.} \end{cases} \tag{2.28}$$

Then the matrix representing the operator A has the singular value decomposition (SVD):

$$A = UDV^T . \tag{2.29}$$

Moore-Penrose Generalized Inverse

Definition 2.30: Let $A : X \to Y$ (X, Y Hilbert spaces) be a bounded linear operator. We say that f is a least squares solution of the equation $Ax = g$ if Af is a best approximation to g from $\mathcal{R}(A)$, that is,

$$\forall x \in X \quad \|Af - g\| \leq \|Ax - g\|.$$

Theorem 2.31: Let P be the orthogonal projection of Y onto $\overline{\mathcal{R}(A)}$. Then the following conditions are equivalent:

(i) f is a least squares solution to $Ax = g$

(ii) $Af = Pg$

(iii) $A^*Af = A^*g$.

Proof: See [17].

A least squares solution does not always exist. We see from Theorem 2.31 that a necessary and sufficient condition for it to exist is $Pg \in \mathcal{R}(A)$. Hence we define the following set

$$W := \{g \in Y : \ Pg \in \mathcal{R}(A)\}.$$

Theorem 2.32: $W = \mathcal{R}(A) \oplus \mathcal{R}(A)^{\perp}$.

Proof: See [17].

Definition 2.33: The Moore-Penrose generalized inverse of A, denoted by $A^{\dagger}$, is the operator with the domain $\mathcal{D}(A^{\dagger}) = \mathcal{R}(A) \oplus \mathcal{R}(A)^{\perp}$ which assigns to each $g \in W$ the minimum norm least squares solution to the equation $Ax = g$.

By Theorem 2.32 the domain of $A^\dagger$ is well-defined. Also since the set of all least squares solutions is convex and closed, it possesses a unique element of minimum norm, so the generalized inverse is well-defined.

The next theorem gives an explicit representation of the Moore-Penrose generalized inverse of a compact operator.

Theorem 2.34: Let $A : X \to Y$ be a compact linear operator. If $g \in \mathcal{D}(A^\dagger)$, then

$$A^\dagger g = \sum_{i \in I} \frac{\langle g, u_i \rangle}{\sigma_i} v_i.$$

Proof: See [5].

Ill-Posedness

Definition 2.35: Let X and Y be Hilbert spaces and consider $A : X \to Y$. The problem

$$A(f) = g \tag{2.36}$$

is well-posed provided that

(i) for any $g \in Y$, there exists a solution $f \in X$ such that $A(f) = g$;

(ii) the solution f is unique;

(iii) the solution f depends continuously on the data g, i.e., suppose f solves $A(f) = g$ and $\bar{f}$ solves $A(\bar{f}) = \bar{g}$, then

$$\|f - \bar{f}\| \to 0 \quad \text{whenever} \quad \|g - \bar{g}\| \to 0.$$

Problem (2.36) is called ill-posed if it is not well-posed.

We discuss the ill-posedness of the problem $Ax = g$, where A is a compact linear operator with infinite dimensional range.

If A is a compact linear operator, A^*A is also compact. If the index set I is an infinite subset of the positive integers, by Theorem 2.21 $\lim_{j \to \infty} \lambda_j = 0$. This also means that

$$\lim_{j \to \infty} \sigma_j = 0. \tag{2.37}$$

Theorem 2.38: Let $A : X \to Y$ be a compact linear operator. $A^\dagger$ is bounded if and only if $\mathcal{R}(A)$ is closed.

Proof: See [17].

Theorem 2.39: Let $A : X \to Y$ be a compact linear operator. $A^\dagger$ is bounded if and only if $dim\mathcal{R}(A) < \infty$.

Proof: If $dim\mathcal{R}(A) < \infty$, then $\mathcal{R}(A)$ is closed, since it is a finite dimensional vector subspace. From Theorem 2.38 $A^\dagger$ is bounded.

Now assume $A^\dagger$ is bounded. Obviously $AA^\dagger = I\,\big|_{\mathcal{R}(A)}$. If $A^\dagger$ is bounded and A is compact, then $AA^\dagger$ is compact. However by the Riesz Lemma [16] an identity operator is compact if and only if its domain is finite dimensional.

Theorem 2.39 shows that the equation $Ax = g$ where A is linear and compact is ill-posed except in trivial cases. The analysis of the general nonlinear case is more complicated. A discussion of the ill-posedness of the system of nonlinear integral equations solved in the thesis is presented in the next chapter.

Tikhonov Regularization

The compact operator equation

$$K(f) = g \tag{2.40}$$

is, except in trivial cases, an ill-posed problem. Therefore its solution cannot be obtained directly. A procedure called Tikhonov regularization is applied. It consists of solving the following problem:

Find a minimum of the functional

$$T_\alpha(f) := \|K(f) - g\|^2 + \alpha J(f), \quad f \in X. \tag{2.41}$$

J is a nonnegative functional on X, called a penalty functional. The scalar α is a positive parameter called the regularization parameter. A solution f_α to this minimization problem is called a regularized solution of the operator equation (2.40).

Example 2.42: Consider $X = H_0^1(\Omega)$ introduced in Example 2.1 (ii) and

$$J(f) = \|f\|^2 = \int_\Omega \nabla f \cdot \nabla f \, dx.$$

This will be the penalty functional actually used in the thesis.

The following two theorems characterize regularized solutions, showing that under certain assumptions they exist. Moreover, an appropriate sequence of regularized solutions converges to the solution of the problem (2.40).

Theorem 2.43: If K is weakly continuous, $J(f)$ is coercive, i.e.,

$$\lim_{\|f\| \to \infty} J(f) = \infty,$$

and weakly lower semicontinuous (for definition and properties see [28]), then there exists an element f_α minimizing the functional (2.41). If $J(f)$ is defined as in Example 2.42, then f_α satisfies

$$\nabla T_\alpha(f) = K'(f)^*(K(f) - g) + \alpha f = 0.$$

Proof: $T_\alpha \geq 0$ so $T_\alpha(X)$ is bounded below by zero and therefore $\inf_{f \in X} T_\alpha(f)$ exists. Denote $m = \inf_{f \in X} T_\alpha(f)$. From the definition of infimum and coercivity of J there exists $\beta \geq 0$ and a sequence $f_k \in X$ such that

$$\lim_{k \to \infty} T_\alpha(f_k) = m \qquad \text{and} \qquad \|f_k\| \leq \beta.$$

Since f_k is bounded we can select a weakly convergent subsequence, i.e.,

$$\exists k_j \quad \exists \bar{f} \qquad f_{k_j} \rightharpoonup \bar{f}.$$

Using the property that the norm in a Hilbert space is weakly lower semicontinuous [28] as well as the assumption that K is weakly continuous and J is weakly lower semicontinuous we have that T_α is weakly lower semicontinuous. Therefore

$$m = \liminf_{j \to \infty} T_\alpha(f_{k_j}) \geq T_\alpha(\bar{f}) \geq m$$

so $\bar{f}$ is a minimizer for (2.41).

Theorem 2.44: Let $g_n \to \bar{g}$ as $n \to \infty$ and assume that $K(f) = \bar{g}$ has the unique solution $\bar{f}$, where K is weakly continuous. If $\alpha = \alpha(n) = \alpha_n$ is chosen so that

$$\lim_{n \to \infty} \alpha(n) = 0 \qquad \text{and} \qquad \frac{\|K(\bar{f}) - g_n\|^2}{\alpha(n)} \to 0,$$

then for f_n minimizing the functional (2.41) with $J(f)$ defined as in Example 2.42 we have $f_n \to \bar{f}$.

Proof: First we show that $f_n \rightharpoonup \bar{f}$. Denote $T_{\alpha(n)}$ by T_n. Since

$$\|f_n\|^2 = \frac{T_n(f_n) - \|K(f_n) - g_n\|^2}{\alpha_n} \leq \frac{T_n(f_n)}{\alpha_n} \leq \frac{T_n(\bar{f})}{\alpha_n}$$
$$= \frac{\|K(\bar{f}) - g_n\|^2}{\alpha_n} + \|\bar{f}\|^2$$

$\{f_n\}$ is bounded. Thus $\{f_n\}$ has a weakly convergent subsequence, i.e.,

$$\exists n_j \quad \exists \hat{f} \in X \qquad f_{n_j} \rightharpoonup \hat{f} \qquad \text{as} \quad j \to \infty.$$

But

$$\|K(f_n) - g_n\|^2 \leq T_n(f_n) \leq T_n(\bar{f}) = \|K(\bar{f}) - g_n\|^2 + \alpha_n \|\bar{f}\|^2 \to 0$$

as $n \to \infty$, since $\alpha_n \to 0$ and $g_n \to \bar{g} = K(\bar{f})$, and hence,

$$\|K(f_n) - \bar{g}\| \leq \|K(f_n) - g_n\| + \|g_n - \bar{g}\| \to 0.$$

Thus

$$\|K(f_{n_j}) - \bar{g}\| \to 0 \quad \text{as} \quad j \to \infty.$$

Now, since $f_{n_j} \rightharpoonup \hat{f}$ we have $K(f_{n_j}) \to K(\hat{f})$ because K is weakly continuous. We also showed that $K(f_{n_j}) \to \bar{g}$. Therefore $K(\hat{f}) = \bar{g}$ and from uniqueness of the solution we get $\hat{f} = \bar{f}$. Thus $f_{n_j} \rightharpoonup \bar{f}$. By the same argument, we can show that any weakly convergent subsequence of $\{f_n\}$ converges weakly to $\bar{f}$. Since $\{f_n\}$ is bounded, $f_n \rightharpoonup \bar{f}$.

Since X is a Hilbert space, the weak convergence together with convergence of $\{\|f_n\|\}$ implies strong convergence [19]. To get convergence of $\{\|f_n\|\}$, consider the inequality

$$\|f_n\|^2 \leq \frac{\|K(\bar{f}) - g_n\|^2}{\alpha_n} + \|\bar{f}\|^2,$$

which yields

$$\liminf_{n\to\infty} \|f_n\| \le \limsup_{n\to\infty} \|f_n\| \le \|\bar{f}\|,$$

since $\dfrac{\|K(\bar{f}) - g_n\|^2}{\alpha_n} \to 0$. Also since the norm in a Hilbert space is weakly lower semicontinuous [28] and $f_n \rightharpoonup \bar{f}$ we have $\|\bar{f}\| \le \liminf_{n\to\infty} \|f_n\|$. Thus $\|f_n\| \to \|\bar{f}\|$ as $n \to \infty$ and, consequently, $f_n \to \bar{f}$.

Tikhonov Regularization in the Linear Case

Let us consider now Tikhonov regularization for $Kf = g$ where K is a compact linear operator. In (2.40) we take $J(f) = \|f\|^2$. This means that we look for a minimizer of the functional

$$T_\alpha(f) = \|Kf - g\|^2 + \alpha\|f\|^2, \quad f \in X. \tag{2.45}$$

From the Examples 2.18 and 2.19 we know that T_α is differentiable and

$$T'_\alpha(f)h = 2\langle Kf - g, Kh\rangle + 2\alpha\langle f, h\rangle = 2\langle K^*(Kf - g) + \alpha f, h\rangle. \tag{2.46}$$

A necessary condition for T_α to have a minimum at f_α is

$$\forall h \in X \quad 2\langle K^*(Kf_\alpha - g) + \alpha f_\alpha, h\rangle = 0$$

$$\text{or} \qquad K^*(Kf_\alpha - g) + \alpha f_\alpha = 0$$

which is equivalent to

$$(K^*K + \alpha I)f_\alpha = K^*g. \tag{2.47}$$

We wish to show that (2.47) is a well-posed problem.

Since by (2.24) K^*K has nonnegative eigenvalues, the Example 2.23 shows that $K^*K + \alpha I$ has all its spectrum contained in $[\alpha, \infty)$, $\alpha > 0$. This means that $0 \notin \sigma(K^*K + \alpha I)$. In other words, the operator $K^*K + \alpha I$ is invertible on X. Therefore (2.47) becomes

$$f_\alpha = (K^*K + \alpha I)^{-1} K^* g. \tag{2.48}$$

Now the Banach Theorem on Isomorphisms (see [16]) states that a continuous linear isomorphism of two vector spaces is a homeomorphism. Therefore $(K^*K + \alpha I)^{-1}$ is continuous and finding a minimum of the Tikhonov functional (2.44) is a well-posed problem.

f_α determined by (2.48) is the minimum of T_α because $T''_\alpha(f) = K^*K + \alpha I$ is a positive definite operator.

Now let $\{v_i\}$ be orthonormal eigenvectors of K^*K and $\{\lambda_i\}$ the associated eigenvalues. For $f(x) = \dfrac{1}{x+\alpha}$ we get, using Theorems 2.21 and 2.22,

$$(K^*K + \alpha I)^{-1} K^* g = f(K^*K) K^* g = \sum_{i \in I} f(\lambda_i) \langle K^* g, v_i \rangle v_i$$

$$= \sum_{i \in I} \frac{1}{\lambda_i + \alpha} \langle g, K v_i \rangle v_i = \sum_{i \in I} \frac{\sigma_i^2}{\sigma_i^2 + \alpha} \frac{\langle g, u_i \rangle}{\sigma_i} v_i =: K_\alpha^\dagger g \tag{2.49}$$

One can prove (see [4] or [5]) that

$$\lim_{\alpha \to 0^+} K_\alpha^\dagger g = K^\dagger g.$$

Linearization of a Nonlinear Problem

When $K : X \to Y$ is nonlinear, we handle the minimization of the functional

$$T_\alpha(f) = \|K(f) - g\|^2 + \alpha \|f\|^2 \tag{2.50}$$

by using a quasi-Newton procedure. We assume that the current approximate minimizer of T_α in (2.50) is f_n and we wish to find a step s_n such that

$$f_{n+1} := f_n + s_n \tag{2.51}$$

is our new approximation. We assume that the affine model of K

$$M(s) := K(f_n) + K'(f_n)s \tag{2.52}$$

describes K in some neighborhood of f_n reasonably well. From Taylor's formula it follows that

$$\|K(f_n + s) - M(s)\| = \|K(f_n + s) - K(f_n) - K'(f_n)s\| \leq C\|s\|^2$$

that is, the error $= O(\|s\|^2)$. The quadratic model for (2.50) becomes

$$m(s) = \|K'(f_n)s + K(f_n) - g\|^2 + \alpha\|f_n + s\|^2 \tag{2.53}$$

Example 2.54: Let $K : X \to Y$ and $K(f)(s) := \int_0^1 k(s,t,f(t))\,dt$ where $\dfrac{\partial k}{\partial f}$ is continuous. Then

$$K(f+h)(s) - K(f)(s) = \int_0^1 \{k(s,t,(f+h)(t)) - k(s,t,f(t))\}\,dt$$

$$= \int_0^1 \{\frac{\partial k}{\partial f}(s,t,f(t))h(t) + R_2(h)\}\,dt$$

where $\|R_2(h)\| \leq C\|h\|^2$. Since

$$0 \leq \lim_{h\to 0} \frac{\|\int_0^1 R_2(h)\,dt\|}{\|h\|} \leq \lim_{h\to 0} \frac{\int_0^1 \|R_2(h)\|\,dt}{\|h\|}$$

$$\leq C \lim_{h\to 0} \frac{\int_0^1 \|h\|^2\,dt}{\|h\|} = C \lim_{h\to 0} \|h\| = 0$$

we have

$$[K'(f)h](s) = \int_0^1 \frac{\partial k}{\partial f}(s,t,f(t))h(t)\,dt. \tag{2.55}$$

In the sequel we will need the gradient and the Hessian of the model (2.53). We derive them here.

Using Examples 2.18 and 2.19 we have

$$m'(s)h = 2\langle K'(f_n)s + K(f_n) - g, K'(f_n)h\rangle + 2\alpha\langle f_n + s, h\rangle$$

so the gradient is

$$G(s) = 2\{K'(f_n)^*(K'(f_n)s + K(f_n) - g) + \alpha(f_n + s)\} \tag{2.56}$$

and the Hessian is obtained easily as

$$H(s) = 2K'(f_n)^* K'(f_n) + 2\alpha I. \tag{2.57}$$

Choice of the Regularization Parameter

So far we have considered the equation $K(f) = g$, in which the right-hand side (the data) was assumed to be known exactly. Denote the solution to this problem by $\hat{f}$. In practice the data usually comes from measurements so it is known approximately, at discrete points only. Taking that into account we arrive at the model equation

$$K(f)(s_i) = g(s_i) + \epsilon_i =: \tilde{g}(s_i) \quad \text{for i=1,2,...,m} \tag{2.58}$$

where the ϵ_i are the errors of measurements taken at $s_1, ..., s_m$.

Minimizing the Tikhonov functional we obtain an approximate solution $\tilde{f}_\alpha$. It is desirable to find α such that $\|\hat{f} - \tilde{f}_\alpha\|$ is as small as possible. One method to estimate such an α is the method of Generalized Cross Validation (GCV). It gives a statistical measure of the magnitude of the residual $\|K\tilde{f}_\alpha - g\|$, which is related to $\|\hat{f} - \tilde{f}_\alpha\|$. By finding $\hat{\alpha}$ which minimizes the GCV functional

$$V(\alpha) = \frac{\|K(\tilde{f}_\alpha) - g\|}{Trace\{I - K'(\tilde{f}_\alpha)[K'(\tilde{f}_\alpha)^* K'(\tilde{f}_\alpha) + \alpha I]^{-1} K'(\tilde{f}_\alpha)\}} \tag{2.59}$$

we estimate the α^* which minimizes the residual.

Theoretical analysis of the GCV method is beyond the scope of the thesis. For references see [13]. The numerical procedure allowing us to find $\hat{\alpha}$ is discussed in Chapter 4.

CHAPTER 3

THE MAGNETIC RELIEF PROBLEM

Experimental evidence suggests that in certain situations variations in the magnetic field of the earth depend primarily on the shape of the boundary between magnetized igneous rock and unmagnetized sediments which cover the rock. One wishes to determine this shape from airborne magnetic data. The mathematical formulation of the relationship between the variations in the magnetic field and the shape and location of the boundary leads to a system of nonlinear first kind integral equations.

Derivation of the System

Let the z-axis be chosen so that the positive z direction is downward, and the measurements of the magnetic field H take place in the plane $z = 0$. Let the boundary surface σ have the parametrization

$$\sigma = \{(x, y, z) : \ z = h + f(x, y), -\infty < x < \infty, -\infty < y < \infty\}. \tag{3.1}$$

We refer to h as the characteristic depth of the surface and we refer to f as the relief function (see Figure 1).

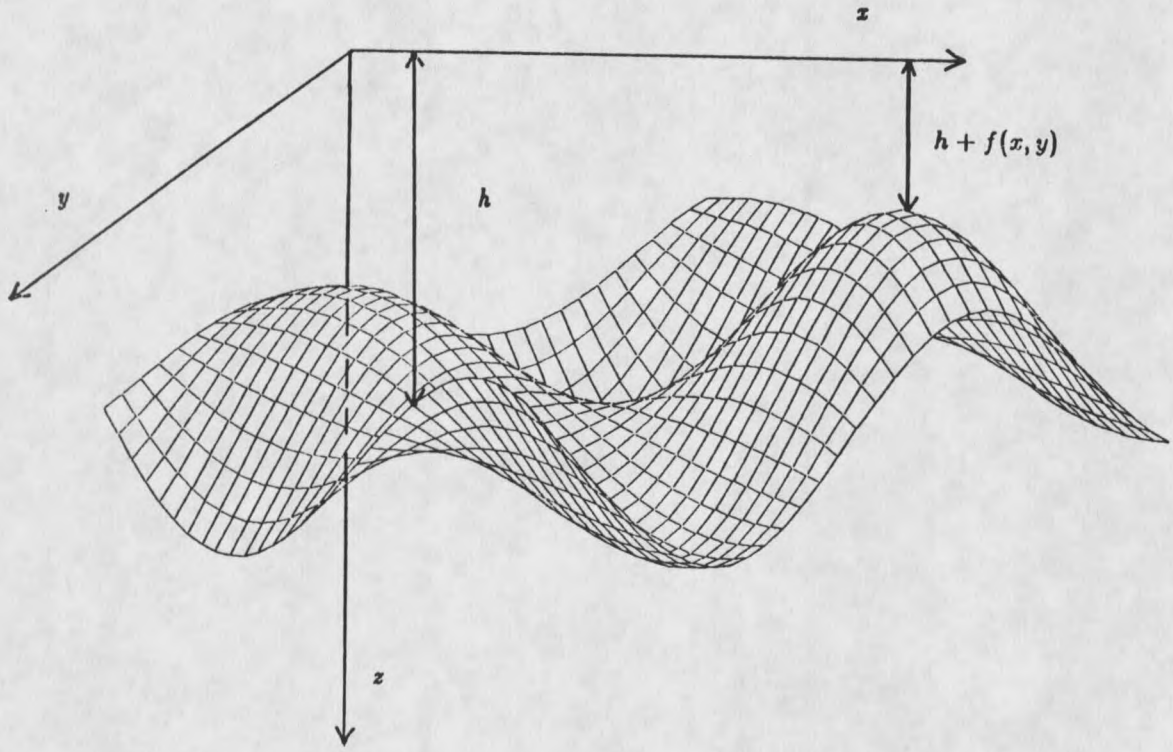


Figure 1. Geometry of the Magnetic Relief Problem

The underlying physical principles are:

(i) Since the magnetic field is produced by microcurrents flowing in the igneous rock, the intensity **H** of the magnetic field can be derived from the scalar magnetic potential U by

$$\mathbf{H} = -\nabla_{\mathbf{p}} U. \tag{3.2}$$

The subscript **p** means that the gradient is taken with respect to the variables (s, t, u) which indicate the position of the point where the field is measured (see

Figure 2).

(ii) The potential at the point $\mathbf{p}$, created by the volume dV of the igneous rock, is

$$dU(\mathbf{p}) = \mathbf{M}(\mathbf{r}) \cdot \nabla_{\mathbf{r}} \frac{1}{\|\mathbf{r} - \mathbf{p}\|} dV. \tag{3.3}$$

Therefore, the total magnetic potential at the point $\mathbf{p}$ is

$$U(\mathbf{p}) = \int_V \mathbf{M}(\mathbf{r}) \cdot \nabla_{\mathbf{r}} \frac{1}{\|\mathbf{r} - \mathbf{p}\|} dV \tag{3.4}$$

where V is the volume occupied by igneous rock. The magnetization vector $\mathbf{M} = [M_x, M_y, M_z]$ has the property

$$div\mathbf{M} = 0 \tag{3.5}$$

(Recall that $div\mathbf{M} = \frac{\partial M_x}{\partial x} + \frac{\partial M_y}{\partial y} + \frac{\partial M_z}{\partial z}$).

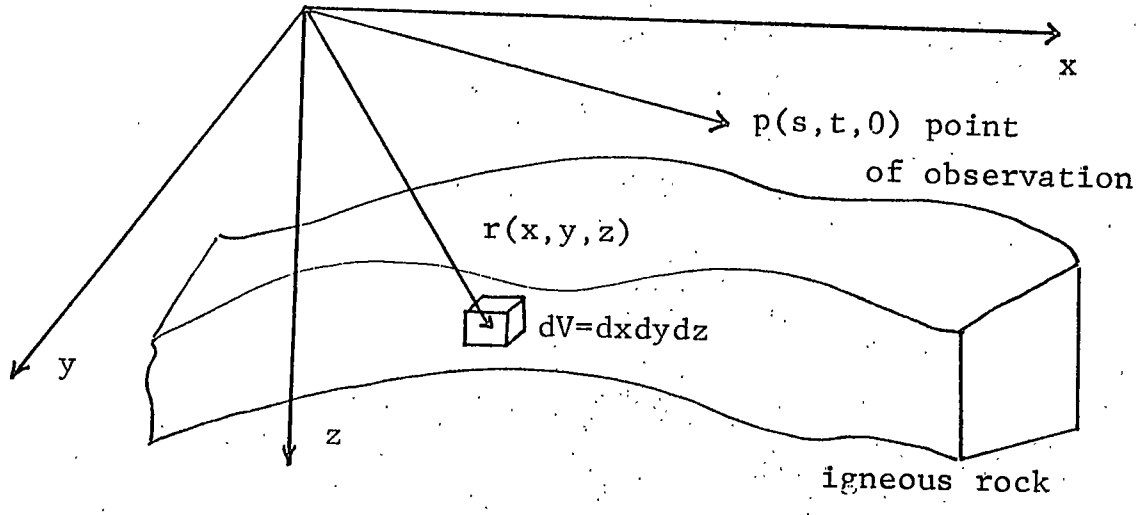


Figure 2. Definition of the Vectors $\mathbf{r}$ and $\mathbf{p}$

Using the identity

$$div(w\mathbf{M}) = \nabla w \cdot \mathbf{M} + w div\mathbf{M} \tag{3.6}$$

where w is any differentiable function we obtain from Stokes' Theorem and (3.4)

$$\begin{aligned} U &= \int_V div_{\mathbf{r}}(\mathbf{M}(\mathbf{r})\frac{1}{\|\mathbf{r}-\mathbf{p}\|})\,dV \\ &= \int_{\partial V} \mathbf{M}(\mathbf{r})\cdot\mathbf{n}\frac{1}{\|\mathbf{r}-\mathbf{p}\|}\,dS, \end{aligned}$$

and consequently, from (3.2)

$$\mathbf{H} = -\int_{\partial V} \mathbf{M}(\mathbf{r})\cdot\mathbf{n}\nabla_{\mathbf{p}}\frac{1}{\|\mathbf{r}-\mathbf{p}\|}\,dS.$$

$\mathbf{n}$ is the outward unit normal to the boundary ∂V of the volume of igneous rock. Because most rock formations are large and extend very deep, the integral can be approximated by an integral over the top surface σ given in (3.1) only. The outward normal $\mathbf{n}$ to the surface σ is

$$\mathbf{n} = \frac{[\frac{\partial f}{\partial x}, \frac{\partial f}{\partial y}, -1]}{\sqrt{(\frac{\partial f}{\partial x})^2 + (\frac{\partial f}{\partial y})^2 + 1}}$$

and

$$dS = dx\,dy\sqrt{1+\left(\frac{\partial f}{\partial x}\right)^2 + \left(\frac{\partial f}{\partial y}\right)^2}.$$

Then the first component of $\mathbf{H} = [H_x, H_y, H_z]$ is

$$\begin{aligned} H_x &= -\int_\sigma (M_x\frac{\partial f}{\partial x} + M_y\frac{\partial f}{\partial y} - M_z)\frac{\partial}{\partial s}\frac{1}{\|\mathbf{r}-\mathbf{p}\|}\,dx\,dy \\ &= -\int_\sigma (M_x\frac{\partial f}{\partial x} + M_y\frac{\partial f}{\partial y} - M_z)\frac{\partial}{\partial s}\frac{1}{\|(x,y,z)-(s,t,0)\|}\,dx\,dy \\ &= \int_\sigma (M_x\frac{\partial f}{\partial x} + M_y\frac{\partial f}{\partial y} - M_z)\frac{x-s}{[(x-s)^2+(y-t)^2+(h+f(x,y))^2]^{\frac{3}{2}}}\,dx\,dy. \end{aligned}$$

If we repeat these calculation for the other two coordinates in an analogous way and let g_x, g_y, g_z denote measurements of the components of $\mathbf{H}$ we obtain the following system of nonlinear first kind integral equations to be solved for f

$$g_x(s,t) = \int_\sigma \frac{(M_x \frac{\partial f}{\partial x} + M_y \frac{\partial f}{\partial y} - M_z)(x-s)}{[(x-s)^2 + (y-t)^2 + (h+f(x,y))^2]^{\frac{3}{2}}}\, dx\, dy \tag{3.7}$$

$$g_y(s,t) = \int_\sigma \frac{(M_x \frac{\partial f}{\partial x} + M_y \frac{\partial f}{\partial y} - M_z)(y-t)}{[(x-s)^2 + (y-t)^2 + (h+f(x,y))^2]^{\frac{3}{2}}}\, dx\, dy \tag{3.8}$$

$$g_z(s,t) = \int_\sigma \frac{(M_x \frac{\partial f}{\partial x} + M_y \frac{\partial f}{\partial y} - M_z)(h+f(x,y))}{[(x-s)^2 + (y-t)^2 + (h+f(x,y))^2]^{\frac{3}{2}}}\, dx\, dy. \tag{3.9}$$

Since the relief function f depends on two variables, we refer to this case as the 2-D magnetic relief problem.

A less realistic but computationally much simpler problem arises when the relief function f is assumed to be independent of the y coordinate. In other words let

$$f(x,y) = f(x)$$

$$\mathbf{M}(x,y,z) = \mathbf{M}(x,y).$$

Then the system (3.7)-(3.9) becomes

$$g_x(s,t) = \int_\sigma (M_x \frac{\partial f}{\partial x} - M_z) \frac{x-s}{[(x-s)^2 + (y-t)^2 + (h+f(x))^2]^{\frac{3}{2}}}\, dx\, dy$$

$$g_y(s,t) = \int_\sigma (M_x \frac{\partial f}{\partial x} - M_z) \frac{y-t}{[(x-s)^2 + (y-t)^2 + (h+f(x))^2]^{\frac{3}{2}}}\, dx\, dy$$

$$g_z(s,t) = \int_\sigma (M_x \frac{\partial f}{\partial x} - M_z) \frac{h+f(x)}{[(x-s)^2 + (y-t)^2 + (h+f(x))^2]^{\frac{3}{2}}}\, dx\, dy$$

Integrating first with respect to y we obtain

$$\begin{aligned} g_x(s,t) &= \int_{-\infty}^{\infty} (M_x \frac{\partial f}{\partial x} - M_z) \{ \int_{-\infty}^{\infty} \frac{x-s}{[(x-s)^2 + (y-t)^2 + (h+f(x))^2]^{\frac{3}{2}}}\, dy \}\, dx \\ &= \int_{-\infty}^{\infty} (M_x \frac{\partial f}{\partial x} - M_z) \frac{2(x-s)}{(x-s)^2 + (h+f(x))^2}\, dx \end{aligned}$$

and analogously

$$g_z(s,t) = \int_{-\infty}^{\infty} (M_x \frac{\partial f}{\partial x} - M_z) \frac{-2(h+f(x))}{(x-s)^2 + (h+f(x))^2}\, dx.$$

$g_y(s,t) = 0$ because the integrand is odd with respect to $t - y$.

One can see that now the components of $\mathbf{g} = [g_x, g_y, g_z]$ do not depend on t and we have a new system

$$g_x(s) = \int_{-\infty}^{\infty} (M_x \frac{\partial f}{\partial x} - M_z) \frac{2(s-x)}{(x-s)^2 + (h+f(x))^2}\, dx \tag{3.10}$$

$$g_z(s) = \int_{-\infty}^{\infty} (M_x \frac{\partial f}{\partial x} - M_z) \frac{-2(h+f(x))}{(x-s)^2 + (h+f(x))^2}\, dx \tag{3.11}$$

If for simplicity we neglect the component g_x, the problem is reduced to a single integral equation with an unknown relief function f, dependent on one variable only, which we refer to as the 1-D magnetic relief problem. The scalar analogue of the system (3.7)-(3.9) is then

$$g_z(s) = -2 \int_{-\infty}^{\infty} \frac{(M_x f'(x) - M_z)(h+f(x))}{(s-x)^2 + (h+f(x))^2}\, dx \tag{3.12}$$

where the integration is now performed over the x-axis.

We will assume that f is identically zero outside a smooth bounded domain Ω, and that measurements of $\mathbf{g}(s,t)$ are taken at points $(s,t) \in \Omega$ only. The components of g can be suitably modified so that the integration above takes place over this restricted domain Ω rather than over the entire x-y plane (or x-axis, in 1-D case). Thus, the problem can be formulated as a nonlinear operator equation (1.1) with

$$K(f) := \int_{\Omega} k(\cdot, x, f(x))\, dx. \tag{3.13}$$

The components of the kernel k are given in the 2-D case by the right-hand sides in (3.7)-(3.9) and in the 1-D case by the right-hand side in (3.12). g is a function whose

components represent measurements of the magnetic field **H**. The characteristic depth h now gives the depth of the surface σ relative to the size of the region Ω.

Ill-Posedness of the Problem

The geophysical problem derived in the previous section has the mathematical form of a system of nonlinear integral first kind equations. More conveniently it can be written as

$$K(f) = g \tag{3.14}$$

with $K(f)$ given by (3.13).

The well-posedness of this particular problem depends on the choice of the spaces X and Y. From the physical point of view it seems appropriate to assume that the solution f is "smooth" in the sense that f is differentiable and $\|f\|^2 := \int_\Omega \nabla f(x) \cdot \nabla f(x)\, dx$ is bounded. Since we have also assumed that f vanishes outside Ω, we choose the Hilbert space X to be $H_0^1(\Omega)$ (Example 2.1 (ii)).

On the other hand the components of **g** come from measurements at discrete points in Ω. One cannot assume that the derivatives of these components are available. Thus an appropriate choice of Y in the 1-D case is $L^2(\Omega)$ (see Example 2.1 (i)). In the 2-D case, since measurements have 3 components, we will consider $Y = [L^2(\Omega)]^3 := L^2(\Omega) \times L^2(\Omega) \times L^2(\Omega)$.

With this physically reasonable choice of spaces X and Y, problem (3.14) is ill-posed. Clearly the components of the kernel k given in the 2-D case by the right-hand sides in (3.7)-(3.9) and in the 1-D case by the right-hand side in (3.12) are continuous, and hence for any $f \in X$, the components of $K(f)$ are continuous (see [19, p 159]). Therefore there exist elements $g \in Y$ for which (3.14) has no

solution. Perhaps a more serious difficulty is that small perturbations in the data $g \in Y$ may give rise to arbitrarily large perturbations in the solution $f \in X$. As Example 2.16 (ii) shows, K is a compact operator with an infinite dimensional range. Therefore the inverse image of an ϵ-neighborhood may have diameter that is arbitrarily large. This means that any stable procedure of finding a solution to (3.14) must involve regularization.

CHAPTER 4

NUMERICAL OPTIMIZATION

To solve the problem (3.14) described in Chapter 3 we need to use a regularization method. The method considered in this thesis is the Tikhonov Regularization method, discussed already in Chapter 2. Since the 2-D case is more complicated we first consider the 1-D case.

1-D Case

To obtain approximate solutions to the ill-posed problem (3.14) with K given by (3.13) and the kernel given by the right-hand side in (3.12) we replace it by a sequence of regularized problems:

Find $f^* \in X$ such that $T_\alpha(f^*) = \min_{f \in X} T_\alpha(f)$ where

$$T_\alpha(f) = \|K(f) - g\|_Y^2 + \alpha \|f\|_X^2 \tag{4.1}$$

and $K : X \to Y$, $X = H_0^1(\Omega)$, $Y = L^2(\Omega)$, and $\Omega = (0,1)$.

The norms $\|\cdot\|_X$ and $\|\cdot\|_Y$ are defined as

$$\|f\|_X = \sqrt{\int_\Omega f'(x)^2 \, dx} \tag{4.2}$$

$$\|g\|_Y = \sqrt{\int_\Omega g^2(x) \, dx}. \tag{4.3}$$

To numerically solve problem (4.1), we must deal with finite dimensional spaces. Thus we introduce the following discretization.

Let $\{\phi_i\}_{i=1}^n$ be a set of basis functions, and define

$X_n = Span\{\phi_1, ..., \phi_n\} \subset X$. For any $f_n \in X_n$,

$$f_n = \sum_{j=1}^{n} c_j \phi_j.$$

$\mathbf{c} := (c_1, ..., c_n)$ is treated as an element of R^n.

The functions $\phi_i(x)$ can be any numerically appropriate basis functions. For example these could be splines (for definition see [30]). The results for the particular geophysical problem described in the thesis are obtained using cubic B-splines.

Given the choice of the ϕ_i's, the discretized version of the (4.2) is obtained as follows:

$$\|f_n\|_X^2 = \int_0^1 f_n'(x)^2\, dx = \int_0^1 (\sum_{i=1}^{n} c_i \phi_i'(x))(\sum_{j=1}^{n} c_j \phi_j'(x))\, dx$$

$$= \sum_{i=1}^{n}\sum_{j=1}^{n} c_i (\int_0^1 \phi_i'(x)\phi_j'(x)\, dx) c_j =: \mathbf{c}^T B_n \mathbf{c}$$

where B_n is a symmetric and positive definite $n \times n$ matrix with entries

$$[B_n]_{i,j} = \int_0^1 \phi_i'(x)\phi_j'(x)\, dx, \quad 1 \le i, j \le n. \tag{4.4}$$

Thus after discretization, the penalty term $\|f\|_X^2$ in (4.1) yields the quadratic form

$$\|f_n\|_X^2 = \mathbf{c}^T B_n \mathbf{c}$$

with B_n defined in (4.4).

Since g comes from measurements and is known at some points $s_1, s_2, ..., s_m$ only, it is natural to introduce the following discretized version $\tilde{\mathbf{g}}$ of g:

$$\tilde{\mathbf{g}} := (g_1, g_2, ..., g_m) \quad \text{where } g_i = g(s_i), \quad \text{for } i = 1, ..., m.$$

We assume $m \ge n$. The norm $\|g\|_Y$ in (4.3) is replaced by the weighted discrete sum

$$\|\tilde{\mathbf{g}}\|^2 := \frac{1}{m}\sum_{i=1}^{m} g_i^2.$$

The discretized version $K_{m\,n} : R^n \to R^m$ of the operator K is

$$[K_{m\,n}(\mathbf{c})]_i := [K(\sum_{j=1}^{n} c_j \phi_j)](s_i), \quad i = 1, ..., m.$$

Thus the finite dimensional analogue of the problem (4.1) is:

Find $\mathbf{c}^* \in R^n$ such that $T_{\alpha,n}(\mathbf{c}^*) = \min_{\mathbf{c} \in R_n} T_{\alpha,n}(\mathbf{c})$ where

$$T_{\alpha,n} := \frac{1}{m} \sum_{i=1}^{m} ([K_{m\,n}(\mathbf{c})]_i - g_i)^2 + \alpha \mathbf{c}^T B_n \mathbf{c}. \tag{4.5}$$

For notational convenience, we drop the subscripts and the tilde, and multiply the objective function in (4.5) by $\frac{m}{2}$. The norm "$\|\cdot\|$" will indicate the usual Euclidean norm in R^n or R^m. Also, since B is symmetric and positive definite, it has a Choleski factorization $B = R^T R$, where R is an upper triangular matrix. Then the objective function for the problem (4.5) becomes

$$T_\alpha(\mathbf{c}) := \frac{1}{2}\{\|K(\mathbf{c}) - \mathbf{g}\|^2 + m\alpha\|R\mathbf{c}\|^2\}. \tag{4.6}$$

2-D Case

In the 2-D case we minimize the objective function T_α in (4.1) with

$$K : X \to Y, \qquad X = H_0^1(\Omega),$$

$$Y = L^2(\Omega) \times L^2(\Omega) \times L^2(\Omega), \quad \text{and} \quad \Omega = (0,1) \times (0,1).$$

We let $\{\psi_j(x,y)\}_{j=1}^N$ be a set of basis functions such that

$$Span\{\psi_1, ..., \psi_N\} = X_N \subset X.$$

For any $f_N \in X_N$

$$f_N(x,y) = \sum_{j=1}^{N} c_j \psi_j(x,y). \tag{4.7}$$

$\mathbf{c} := (c_1, ..., c_N)$ is treated as an element of R^N.

In the thesis the two-dimensional basis functions ψ_j were taken to be the tensor products of the one-dimensional basis functions ϕ_i, i.e., each $\psi(x,y)$ is a product of two one dimensional basis functions $\phi(x)$ and $\phi(y)$. To be more exact, we need to introduce some ordering. We will assume the following:

$$
\begin{aligned}
\psi_1(x,y) &= \phi_1(x)\phi_1(y) \\
\psi_2(x,y) &= \phi_2(x)\phi_1(y) \\
&\vdots \\
\psi_n(x,y) &= \phi_n(x)\phi_1(y) \\
\psi_{n+1}(x,y) &= \phi_1(x)\phi_2(y) \\
&\vdots \\
\psi_N(x,y) &= \phi_n(x)\phi_n(y)
\end{aligned}
\tag{4.8}
$$

where $N = n^2$. Thus (4.7) can be represented as

$$f_N(x,y) = \sum_{i=1}^{n}\sum_{j=1}^{n} d_{ij}\phi_i(x)\phi_j(y)$$

with coefficients d_{ij} equated to appropriate coefficients c_k in (4.7).

The norm

$$\|f\|_X = \left\{ \int_0^1 \int_0^1 \left[\left(\frac{\partial f}{\partial x}(x,y) \right)^2 + \left(\frac{\partial f}{\partial y}(x,y) \right)^2 \right] dx\, dy \right\}^{\frac{1}{2}}$$

becomes after discretization

$$\begin{aligned}
\|f_N\|_X^2 &= \int_0^1 \int_0^1 \left[\left(\frac{\partial f_N}{\partial x}(x,y) \right)^2 + \left(\frac{\partial f_N}{\partial y}(x,y) \right)^2 \right] dx\, dy \\
&= \int_0^1 \int_0^1 \left[\left(\frac{\partial}{\partial x} \sum_{k=1}^{N} c_k \psi_k(x,y) \right)^2 + \left(\frac{\partial}{\partial y} \sum_{k=1}^{N} c_k \psi_k(x,y) \right)^2 \right] dx\, dy \\
&= \int_0^1 \int_0^1 \left[\left(\sum_{k=1}^{N} c_k \phi'_{i(k)}(x) \phi_{j(k)}(y) \right)^2 + \right. \\
&\qquad \left. \left(\sum_{k=1}^{N} c_k \phi_{i(k)}(x) \phi'_{j(k)}(y) \right)^2 \right] dx\, dy \\
&= \sum_{k=1}^{N} \sum_{l=1}^{N} c_k \left(\int_0^1 \phi'_{i(k)}(x) \phi'_{p(l)}(x)\, dx \int_0^1 \phi_{j(k)}(y) \phi_{q(l)}(y)\, dy + \right. \\
&\qquad \left. \int_0^1 \phi_{i(k)}(x) \phi_{p(l)}(x)\, dx \int_0^1 \phi'_{j(k)}(y) \phi'_{q(l)}(y)\, dy \right) c_l \\
&=: \mathbf{c}^T B_N \mathbf{c}
\end{aligned}$$

where B_N is a symmetric positive definite matrix with entries

(4.9)

$$\begin{aligned}
[B_N]_{kl} &= \int_0^1 \phi'_{i(k)}(x) \phi'_{p(l)}(x)\, dx \int_0^1 \phi_{j(k)}(y) \phi_{q(l)}(y)\, dy \\
&\quad + \int_0^1 \phi_{i(k)}(x) \phi_{p(l)}(x)\, dx \int_0^1 \phi'_{j(k)}(y) \phi'_{q(l)}(y)\, dy, \quad 1 \le k, l \le N
\end{aligned}$$

and the subscripts of the one-dimensional basis functions ϕ depend on the subscript of the two dimensional basis function ψ. In the case of the ordering (4.8)

$$k = n(j-1) + i \quad \text{and} \quad i(k) = k - n\left[\frac{k-1}{n} \right], \quad j(k) = \left[\frac{k-1}{n} \right] + 1.$$

$[\cdot]$ denotes the greatest integer function. Thus in the 2-D case the penalty term $\|f\|_X^2$ in (4.1) yields, after discretization, the quadratic form

$$\|f_N\|_X^2 = \mathbf{c}^T B_N \mathbf{c}$$

with B_N defined now in (4.9).

In the 2-D case we are presented with three equations (3.7)-(3.9) with left hand sides g_x, g_y, g_z corresponding to the measurements of the components of the magnetic field. If we assume that the measurements are taken at the points $s_1, s_2, ..., s_{m^2} \in \Omega = (0,1) \times (0,1)$ such that

$$(s_1, ..., s_{m^2}) = \big((t_1, t_1), (t_2, t_1), ..., (t_m, t_1), ..., (t_m, t_m)\big),$$

then g will be represented by the $M = 3m^2$ dimensional vector $\tilde{\mathbf{g}}$

$$\begin{aligned}\tilde{\mathbf{g}} &= (g_x(s_1), ..., g_x(s_{m^2}), g_y(s_1), ..., g_y(s_{m^2}), g_z(s_1), ..., g_z(s_{m^2})) \\ &= (g_1, ..., g_M) \in R^M.\end{aligned}$$

The norm $\|g\|_Y$ in (4.3) is replaced, as in 1-D case, by the weighted discrete sum

$$\|\mathbf{g}\|^2 := \frac{1}{M} \sum_{i=1}^{M} g_i^2.$$

If we call the right-hand sides of (3.7)-(3.9) K_x, K_y, K_z respectively, then the

discretized version $K_{M\,N} : R^N \to R^M$ of the operator K becomes

$$K_{M\,N}(\mathbf{c}) := \begin{pmatrix} [K_x(\sum_{j=1}^{N} c_j\psi_j)](s_1) \\ \vdots \\ [K_x(\sum_{j=1}^{N} c_j\psi_j)](s_{m^2}) \\ [K_y(\sum_{j=1}^{N} c_j\psi_j)](s_1) \\ \vdots \\ [K_y(\sum_{j=1}^{N} c_j\psi_j)](s_{m^2}) \\ [K_z(\sum_{j=1}^{N} c_j\psi_j)](s_1) \\ \vdots \\ [K_z(\sum_{j=1}^{N} c_j\psi_j)](s_{m^2}). \end{pmatrix}$$

Thus in the 2-D case, although details become more complicated, we still obtain a finite dimensional analogue of the problem (4.1) which is similar to (4.5) in the 1-D case.

Globally Convergent Minimization Algorithm

In order to minimize T_α defined in (4.6) a quasi-Newton method together with a trust region approach is applied. We move in a descent direction, which is determined by a quasi-Newton step unless the length of the step is greater than the size of the region in which we believe that the functional is well described

by its quadratic model. In that case the solution to a constrained minimization problem determines the step. Because the possibility of taking the unconstrained quasi-Newton step is checked first, the procedure retains fast local convergence.

We replace the objective functional T_α in (4.6) with its quadratic model (compare Linearization of a Nonlinear Problem, Chapter 2)

$$m(\mathbf{s}) = \frac{1}{2}\{\|K'(\mathbf{c}_k)\mathbf{s} + K(\mathbf{c}_k) - \mathbf{g}\|^2 + \alpha\|R(\mathbf{c}_k + \mathbf{s})\|^2\}.$$

Consider the iteration

$$\mathbf{c}_{k+1} := \mathbf{c}_k + \mathbf{s},$$

where $\mathbf{c}_k$ is the current approximate minimizer of T_α and $\mathbf{s}$ is the minimizer of the current model m. Now the necessary condition for a minimum of m becomes (see (2.47))

$$\begin{aligned} m'(\mathbf{s}) &= K'(\mathbf{c}_k)^T[K'(\mathbf{c}_k)\mathbf{s} + K(\mathbf{c}_k) - \mathbf{g}] + \alpha R^T R(\mathbf{c}_k + \mathbf{s}) \\ &= K'(\mathbf{c}_k)^T[K'(\mathbf{c}_k)\mathbf{s} + K(\mathbf{c}_k) - \mathbf{g}] + \alpha B(\mathbf{c}_k + \mathbf{s}) = 0. \end{aligned}$$

Therefore, solving for s,

$$\mathbf{c}_{k+1} = \mathbf{c}_k - [K'(\mathbf{c}_k)^T K'(\mathbf{c}_k) + \alpha B]^{-1}\{K'(\mathbf{c}_k)^T[K(\mathbf{c}_k) - \mathbf{g}] + \alpha B\mathbf{c}_k\}. \tag{4.10}$$

The approach above is equivalent to the following quasi-Newton method [15]. A necessary condition for (4.6) to have minimum, the gradient equal to zero, is

$$G(\mathbf{c}) := K'(\mathbf{c})^T[K(\mathbf{c}) - \mathbf{g}] + \alpha B\mathbf{c} = 0. \tag{4.11}$$

The Hessian of the objective function is

$$H(\mathbf{c}) := K''(\mathbf{c})^T[K(\mathbf{c}) - \mathbf{g}] + K'(\mathbf{c})^T K'(\mathbf{c}) + \alpha B. \tag{4.12}$$

To solve the equation $G(\mathbf{c}) = 0$ by the Newton method we would consider the iteration

$$\mathbf{c}_{k+1} = \mathbf{c}_k - H(\mathbf{c}_k)^{-1} G(\mathbf{c}_k), \quad k = 0, 1, \ldots .$$

Due to expense in computing $K''(\mathbf{c})$, the Hessian is approximated by the symmetric positive definite matrix

$$\hat{H}(\mathbf{c}) := K'(\mathbf{c})^T K'(\mathbf{c}) + \alpha B \tag{4.13}$$

and the quasi-Newton iteration

$$\mathbf{c}_{k+1} = \mathbf{c}_k - \hat{H}(\mathbf{c}_k)^{-1} G(\mathbf{c}_k), \quad k = 0, 1, \ldots \tag{4.14}$$

is equivalent to (4.10).

It should be noticed that the quasi-Newton step $\mathbf{s} = -\hat{H}(\mathbf{c}_k)^{-1} G(\mathbf{c}_k)$ is in a descent direction of the model m. By a descent direction we mean a direction s such that

$$m(\mathbf{c}_k + \mathbf{s}) \leq m(\mathbf{c}_k).$$

s is a descent direction if it satisfies

$$\mathbf{s}^T \nabla m < 0.$$

In our case we have

$$\left[-\hat{H}(\mathbf{c}_k)^{-1} G(\mathbf{c}_k)\right]^T G(\mathbf{c}_k) = -G(\mathbf{c}_k)^T \{\hat{H}(\mathbf{c}_k)^{-1}\}^T G(\mathbf{c}_k) < 0,$$

since $\hat{H}(\mathbf{c}_k)$ symmetric and positive definite implies $\{\hat{H}(\mathbf{c}_k)^{-1}\}^T$ is positive definite as well.

The quasi-Newton method (4.14) will converge to the local minimizer $\mathbf{c}^*$ of (4.6) provided $H(\mathbf{c}^*)$ is positive definite and the initial guess $\mathbf{c}_0$ is sufficiently close

to $\mathbf{c}^*$. Otherwise, the iteration may not converge or it may converge to a solution of $G(\mathbf{c}) = 0$ which is not a local minimizer. To obtain convergence to a minimizer under much weaker conditions, a trust region approach [15] is used. Iteration (4.14) is replaced by

$$\mathbf{c}_{k+1} = \mathbf{c}_k + \mathbf{s}_k \tag{4.15}$$

where $\mathbf{s}_k$ solves the constrained minimization problem

$$\min_{\mathbf{s} \in R^n} \frac{1}{2}\{\|K(\mathbf{c}_k) + K'(\mathbf{c}_k)\mathbf{s} - \mathbf{g}\|^2 + \alpha\|R(\mathbf{c}_k + \mathbf{s})\|^2\} \tag{4.16}$$

$$\text{subject to } \|R\mathbf{s}\| \leq \delta_k,$$

and the trust region radius δ_k is chosen to obtain sufficient decrease in $T_\alpha(\mathbf{c})$ at each iteration to guarantee convergence.

To solve the problem (4.16), we first diagonalize it using the Singular Value Decomposition (SVD). Consider first the change of variables $\tilde{\mathbf{s}} = R\mathbf{s}$. Then the objective function in (4.16) becomes

$$\frac{1}{2}\{\|A\tilde{\mathbf{s}} - \mathbf{b}\|^2 + \alpha\|\tilde{\mathbf{c}} + \tilde{\mathbf{s}}\|^2\}$$

where $A := K'(\mathbf{c}_k)R^{-1}$, $\mathbf{b} := \mathbf{g} - K(\mathbf{c}_k)$, and $\tilde{\mathbf{c}} := R\mathbf{c}_k$. Let A have the following SVD:

$$A = UDV^T, \quad U_{m\times m}, V_{n\times n} \text{ orthogonal},$$

and

$$[D_{m\times n}]_{ij} = \begin{cases} \sigma_i, & \text{if } i = j \text{ and } i \leq n; \\ 0, & \text{otherwise,} \end{cases}$$

where the σ_i are the singular values introduced in Definition 2.27, and consider the second change of variables

$$\hat{\mathbf{s}} = V^T\tilde{\mathbf{s}}. \tag{4.17}$$

Since U is orthogonal, $\|Ux\| = \|x\|$ and $U^{-1} = U^T$, and the same holds for V, we obtain the diagonalized problem

$$\min_{\hat{s}\in R^n} \frac{1}{2}\{\|D\hat{s} - \hat{b}\|^2 + \alpha\|\hat{c} + \hat{s}\|^2\} \tag{4.18}$$

$$\text{subject to } \|\hat{s}\|^2 \leq \delta_k^2,$$

where $\hat{c} := V^T R c_k$, $\hat{b} := U^T b$, which is equivalent to (4.16).

The theory of constrained minimization allows us to find the unique solution to (4.18). If the norm of the minimizer of (4.18) is less than δ_k then the constraint is not active (does not play a role). Otherwise, by the Kuhn-Tucker criterion [31], there exists a Lagrange multiplier $\mu \geq 0$ such that

$$D^T(D\hat{s} - \hat{b}) + \alpha(\hat{c} + \hat{s}) + \mu\hat{s} = 0.$$

$\hat{s}$ is found in terms of μ

$$\hat{s}(\mu) = \{D^T D + (\alpha + \mu)I\}^{-1}(D\hat{b} - \alpha\hat{c}) \tag{4.19}$$

and substituted to the active constraint, $\|\hat{s}\|^2 = \delta_k^2$, yielding the equation for μ

$$g(\mu) := \|\hat{s}(\mu)\|^2 - \delta_k^2 = 0. \tag{4.20}$$

Notice that the inverse operator in (4.19) always exists because $\alpha + \mu > 0$. Clearly, if the constraint is not active then

$$s = R^{-1}V\hat{s}(0)$$

solves the minimization problem (4.16), otherwise

$$s = s(\mu) = R^{-1}V\hat{s}(\mu).$$

The idea of the trust region approach can be described in the following way. Instead of minimizing the functional T_α in (4.6) the minimization of its model around the current point $\mathbf{c}_k$ is considered. Depending on the geometry of the level curves of T_α, the model is adequate in a smaller or bigger neighborhood of $\mathbf{c}_k$. This determines what length of the step $\|\mathbf{s}_k\|$ from $\mathbf{c}_k$ to $\mathbf{c}_{k+1}$ is acceptable to create a globally convergent procedure. We are then led to the following algorithm.

For $k = 1, 2, \ldots$ do

1. Find the quasi-Newton step $\hat{\mathbf{s}}(0)$
2. If $\|\hat{\mathbf{s}}(0)\| \leq \delta_k$ then go to 5, else
3. Approximately solve $\|\hat{\mathbf{s}}(\mu)\|^2 - \delta_k^2 = 0$ for μ.
4. Find $\hat{\mathbf{s}}(\mu)$ and compute $\mathbf{s}(\mu) = R^{-1}V\hat{\mathbf{s}}(\mu)$.
5. Decide whether $\mathbf{c}_{k+1} = \mathbf{c}_k + \mathbf{s}_k(\mu)$ is an acceptable new approximation.

   If yes go to 7, else
6. Decrease the trust region radius δ_k, go to 3
7. If the stopping criteria are satisfied, then END, else
8. Find δ_{k+1}, i.e., retain, increase or reduce δ_k, go to 1

To do step 3, i.e., to solve (4.20) approximately we used the so called "hook" method described in [15,p 134], which requires $g(\mu)$ and its derivative $g'(\mu)$. In terms of the singular values σ_i and the components of $\hat{\mathbf{b}}$ and $\hat{\mathbf{c}}$,

$$g(\mu) = \sum_{i=1}^{n} \left[\frac{\sigma_i \hat{b}_i - \alpha \hat{c}_i}{\sigma_i^2 + \alpha + \mu} \right]^2 - \delta_k^2, \tag{4.21}$$

so both $g(\mu)$ and $g'(\mu)$ can be obtained easily.

The condition for accepting the new iterate $\mathbf{c}_{k+1}$ in step 5 and the method of reducing the new trust region radius δ_k in step 6 are described in [15,p 144]. The

basic idea is to obtain sufficient decrease in the objective function T_α, i.e., so that

$$T_\alpha(\mathbf{c}_k + \mathbf{s}) \leq T_\alpha(\mathbf{c}_k) + \epsilon \nabla T_\alpha(\mathbf{c}_k)^T \mathbf{s} \tag{4.22}$$

where ϵ is a small positive parameter and $\nabla T_\alpha(\mathbf{c}_k)^T \mathbf{s} < 0$ since $\mathbf{s}$ is in a descent direction. We used $\epsilon = 10^{-4}$, so that the condition (4.22) was hardly more stringent than $T_\alpha(\mathbf{c}_k + \mathbf{s}) \leq T_\alpha(\mathbf{c}_k)$. If the condition (4.22) is not satisfied, we reduce the trust region radius by a factor between $\frac{1}{10}$ and $\frac{1}{2}$ in step 6 and return to step 3. The reduction factor is determined by finding the minimum of the quadratic model that fits $T_\alpha(\mathbf{c}_k)$, $T_\alpha(\mathbf{c}_{k+1})$ and the directional derivative $\nabla T_\alpha(\mathbf{c}_k)^T \mathbf{s}$. We then let the new trust radius δ_{k+1} extend to the minimizer of this model.

If the condition (4.22) is satisfied, and the last step was not a quasi-Newton step, we still compare the actual reduction in the objective function with the predicted one. Good agreement probably means that the current δ_k is an underestimate of the radius in which our model adequately describes the objective function. So rather then move directly to $\mathbf{c}_{k+1}$, we save it, double the δ_k and find the new step using the current model. If the new step does not satisfy the condition (4.22) we drop back to the old $\mathbf{c}_{k+1}$ but otherwise we consider doubling δ_k again. This may save a significant number of gradient computations.

In step 8 of the algorithm we update δ_k allowing three possibilities: doubling, halving, or retaining the current value. If the quadratic model predicts the actual objective function reduction sufficiently well, we take $\delta_{k+1} = 2\delta_k$. If the model greatly overestimates the decrease in T_α, we take $\delta_{k+1} = \delta_k/2$. Otherwise $\delta_{k+1} = \delta_k$. This approach allows us to increase the size of the step whenever it is possible, thereby decreasing the number of iterations needed to minimize T_α.

The GCV functional in (2.59), used to estimate the optimal regularization

parameter α, is computed using

$$V(\alpha) = \frac{\frac{1}{m}\|K(\mathbf{c}_\alpha) - \mathbf{g}\|^2}{[\frac{m-n}{m} + \sum_{i=1}^{n} \frac{\alpha}{\sigma_i^2 + m\alpha}]^2}, \tag{4.23}$$

where $\mathbf{c}_\alpha$ minimizes the objective function (4.6).

The approach presented in this thesis is numerically stable, quite efficient, and it allows easy computation of the GCV functional $V(\alpha)$. The singular values σ_i can also be used to obtain (linearized) stability estimates. They are used in the next section to quantify the "degree of ill-posedness" of the magnetic relief problem.

CHAPTER 5

NUMERICAL RESULTS FOR MAGNETIC RELIEF PROBLEM

The numerical results for the 1-D and the 2-D magnetic relief problems described in Chapter 3 are presented. The computations for the 1-D problem were performed on a Zenith (IBM-compatible) PC. The 2-D problem is conceptually quite similar to the 1-D problem but computationally much more difficult due to two dimensional integration and the greater number of basis functions required to represent the solution. The 2-D computations were performed on the CRAY X-MP supercomputer located at the San Diego Supercomputer Center.

For computational purposes the domain of the operator K in (2.40) was taken to be $\Omega = (0,1)$ in 1-D case and $\Omega = (0,1) \times (0,1)$ in 2-D case, and the magnetization vector was $\mathbf{M} = [M_x, M_y, M_z]^T = [1,1,1]^T$.

Linearized Stability Analysis

From physical arguments, one might expect quite accurate numerical solutions for small characteristic depth h, and more difficulty in recovering the shape of the relief function for increasing h. Numerically this corresponds to solving a system for which ill-conditioning increases as the depth h increases. Since

$$K(f + \Delta f) \approx K(f) + K'(f)\Delta f \tag{5.1}$$

the derivative operator $K'(f)$ was analyzed.

In the 1-D case, the derivative operator $K'(f) : X \to Y$ is defined by

$$(K'(f)u)(s) = 2\int_\Omega \frac{-h - f(x)}{(s-x)^2 + (h+f(x))^2} M_x u'(x)dx$$

$$+2\int_\Omega (M_x f'(x) - M_x)\frac{-(s-x)^2 + (h+f)^2}{[(s-x)^2 + (h+f(x))^2]^2} u(x)dx.$$

The derivative is expressed as the sum of two linear integral operators. Given $u \in H^1(\Omega)$, the first is applied to $u'(x)$ while the second is applied to $u(x)$. Figure 3 shows plots of minus one-half the kernel of the first term of $K'(f)$ for depth $h = 0.1$ and 0.2 (solid and dotted line respectively) at fixed s and at $f = 0$. Figure 4 corresponds to minus one half the kernel of the second term of $K'(f)$. One sees from these two plots that the kernels become more "flat" and less "delta-like" as the depth h increases.

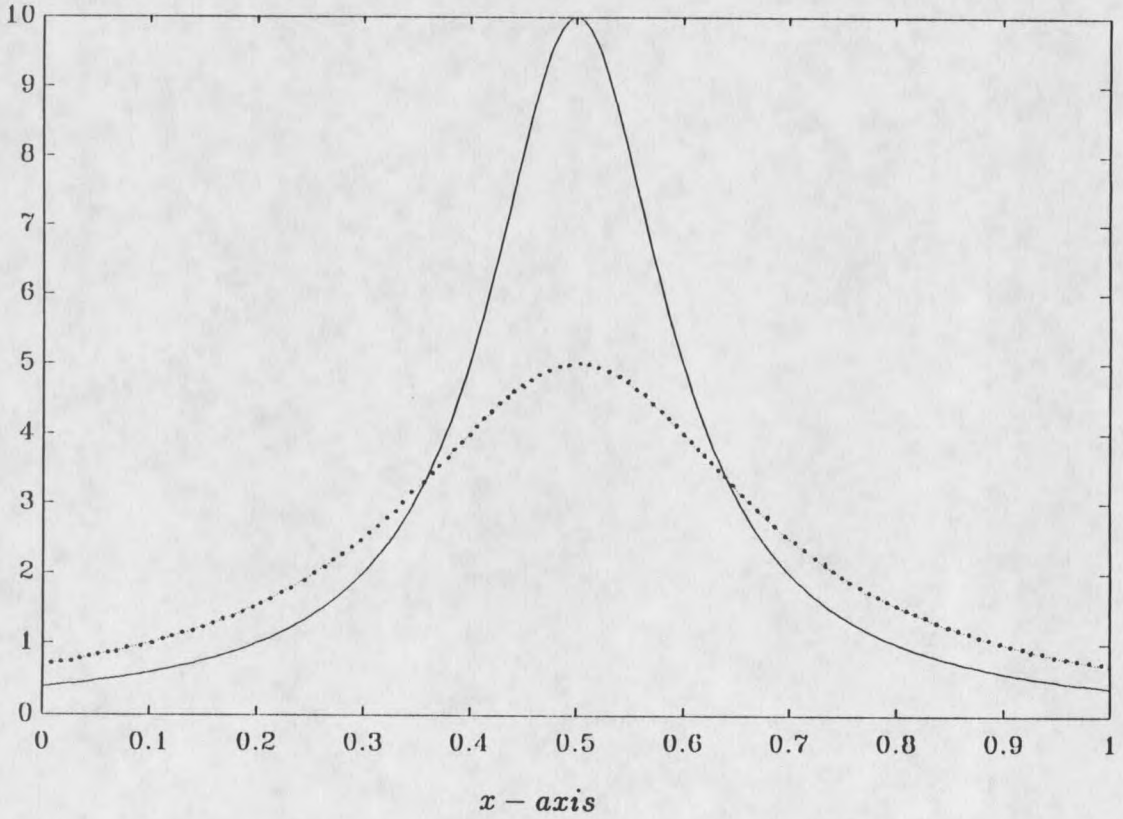


Figure 3. Derivative Kernel $\frac{\partial k_s}{\partial f'}$ for $h = 0.1$ and $h = 0.2$.

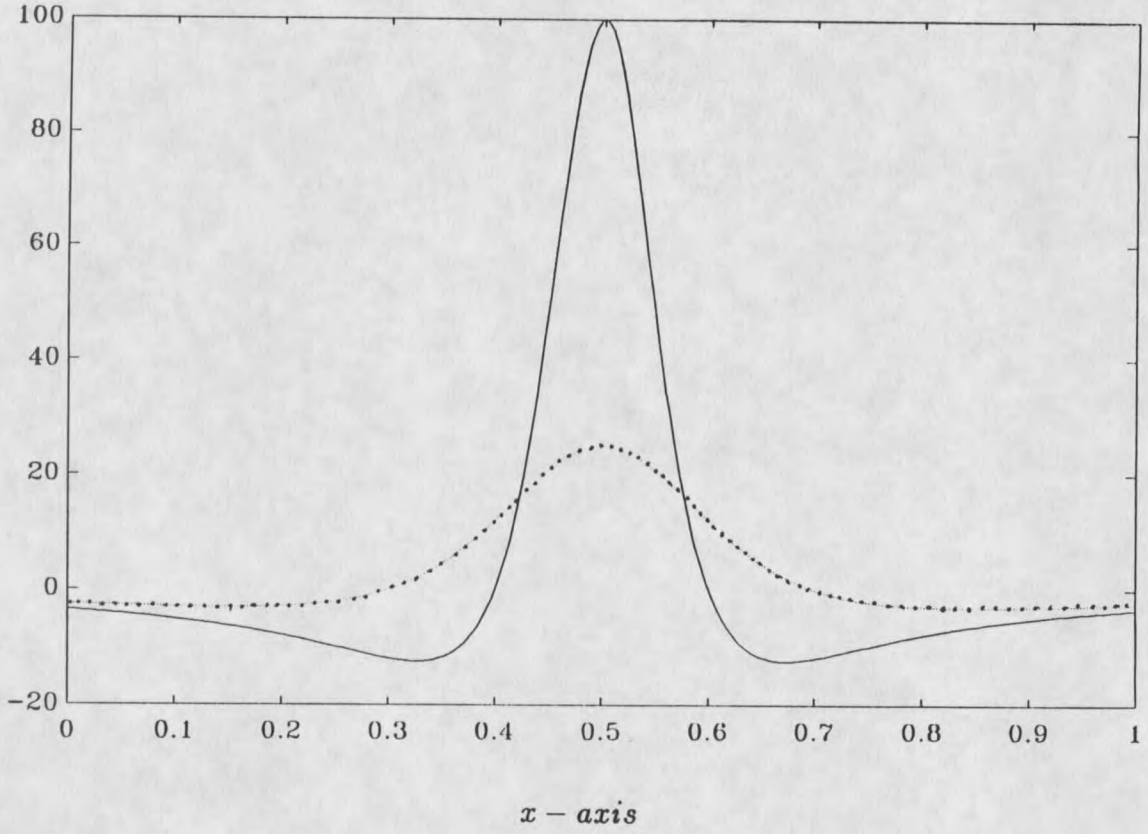


Figure 4. Derivative Kernel $\frac{\partial k_x}{\partial f}$ for $h = 0.1$ and $h = 0.2$.

A quantitative description of how increasing depth reduces the resolution is given in Figures 5. It shows singular values in order of decreasing magnitude for both $h = 0.1$ (stars) and $h = 0.2$ (circles) for the first term of $K'(f)$. Singular values appear to decay exponentially (note logarithmic scale), i.e., the ith singular value σ_i appears to be

$$\sigma_i \approx c \ \exp(-i\beta), \quad i = 1, 2..., \quad c > 0, \ \beta > 0.$$

As the depth h increases, the constant β increases. Thus the singular values decay

more rapidly in case of greater characteristic depth h. This causes the unregularized linear operator $K'(f)$ on the right hand side of (5.1) to possess a larger condition number.

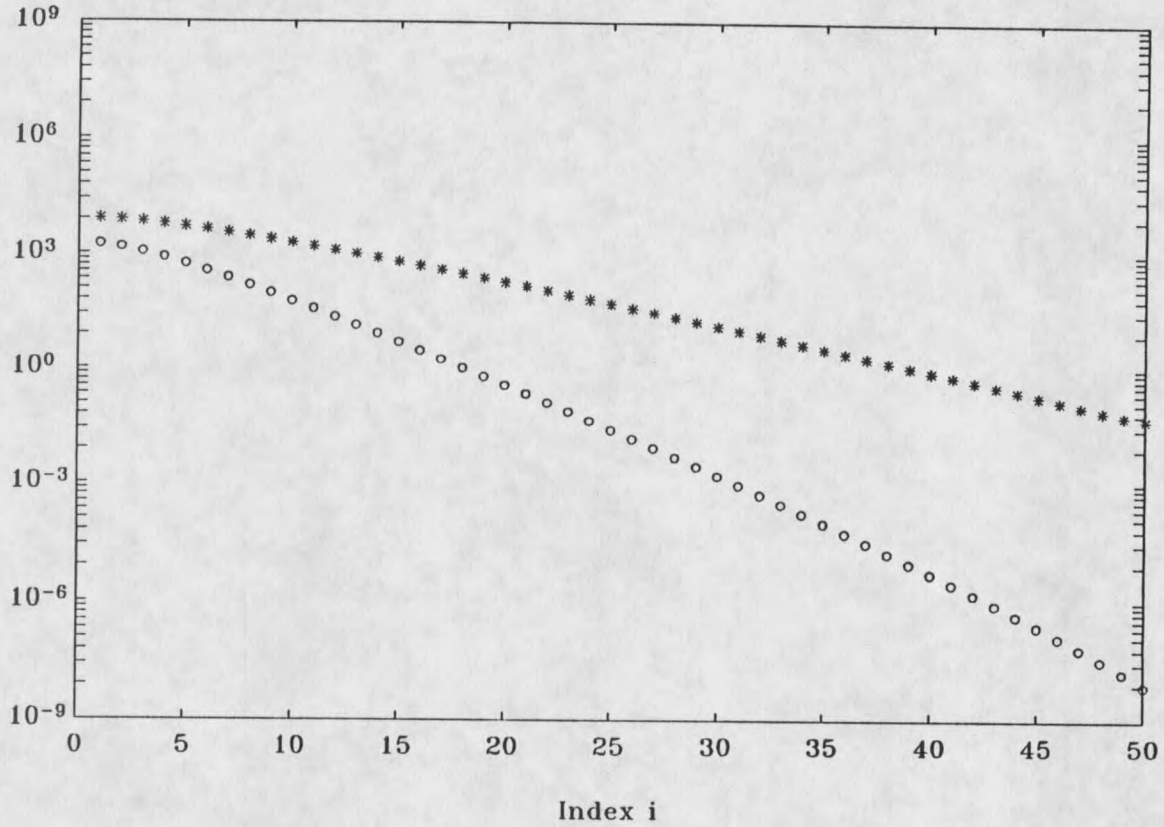


Figure 5. Singular Values of the Derivative

Tikhonov Regularization filters out the components of solution related to small singular values. Therefore it comes as no surprise that the amount of detail the numerical solution may possess decreases with increasing h. A similar analysis was done for the 2-D case. Since the results are analogous to the 1-D case the graphs are not presented here.

Computational Results

To obtain approximate solution to (3.9) and (3.12) using the implementation of Tikhonov Regularization described in Chapter 4 we generated synthetic data

$$g_i = K(f)(s_i).$$

The true magnetic relief function was taken to be linear combination of Gaussians. In 1-D case

$$f(x) = a_1 \ exp(-d_1(x - x_1)^2) + a_2 \ exp(-d_2(x - x_2)^2).$$

The parameters $a_1 = 0.05$, $a_2 = 0.025$ control the magnitude of the solution. $d_1 = 60$, $d_2 = 40$ determine the rate of decay of the Gaussians, and $x_1 = 0.33$, $x_2 = 0.66$ specify the location of the peaks. We generated $m = 50$ data points $g_i = g(s_i)$, $s_i = \frac{i}{m-1}$, $i = 0, 1, ..., m-1$. To the data g_i we added a pseudo-random error vector $\epsilon \sim N(0, \sigma^2 I)$, i.e., the components ϵ_i of the error vector are independent, identically distributed Gaussian random variables which satisfy

$$E(\epsilon_i) = 0 \quad \text{and} \quad E(\epsilon_i \epsilon_j) = \begin{cases} \sigma^2, & i = j, \\ 0, & i \neq j, \end{cases} \quad 1 \leq i, j \leq m.$$

$E(\cdot)$ denotes mathematical expectation. The standard deviation σ was picked so that

$$\frac{\sqrt{E\|\epsilon\|^2}}{\|g\|} = 0.01.$$

We used $n = 20$ piecewise cubic spline (B-spline) basis functions ϕ_j, each satisfying the boundary conditions $\phi_j(0) = \phi_j(1) = 0$ to approximate the true solution. The resulting finite dimensional minimization problem (4.6) was solved for a decreasing sequence of regularization parameters $\alpha = 10^{-p}, p = 0, 1, ..., 5$.

The approximations obtained for $h = 0.1$ are shown in Figure 6, and for $h = 0.2$ in Figure 7. In both pictures the +'s represent the true solution, the o's represent the regularized solution for $\alpha = 1.0$, the solid curve represents the regularized solution for $\alpha = 0.1$, and the dotted curve represents the regularized solution for $\alpha = 10^{-5}$. These results show that on one hand the numerical solution improves, as it should, for decreasing values of the regularization parameter α but on the other hand too small values give rise to the oscillations in the solution for the error contaminated data. This behavior is more strongly demonstrated for bigger depth h.

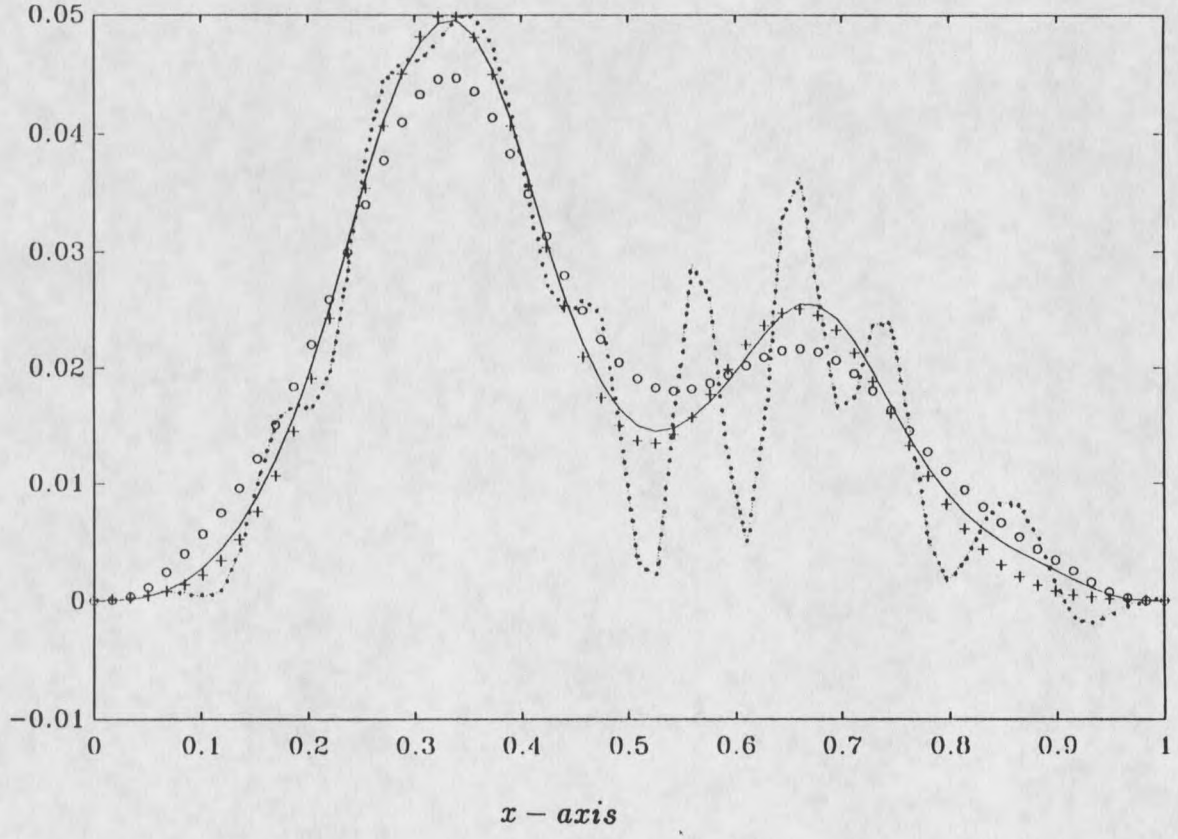


Figure 6. Approximate Solutions for $h = 0.1$.

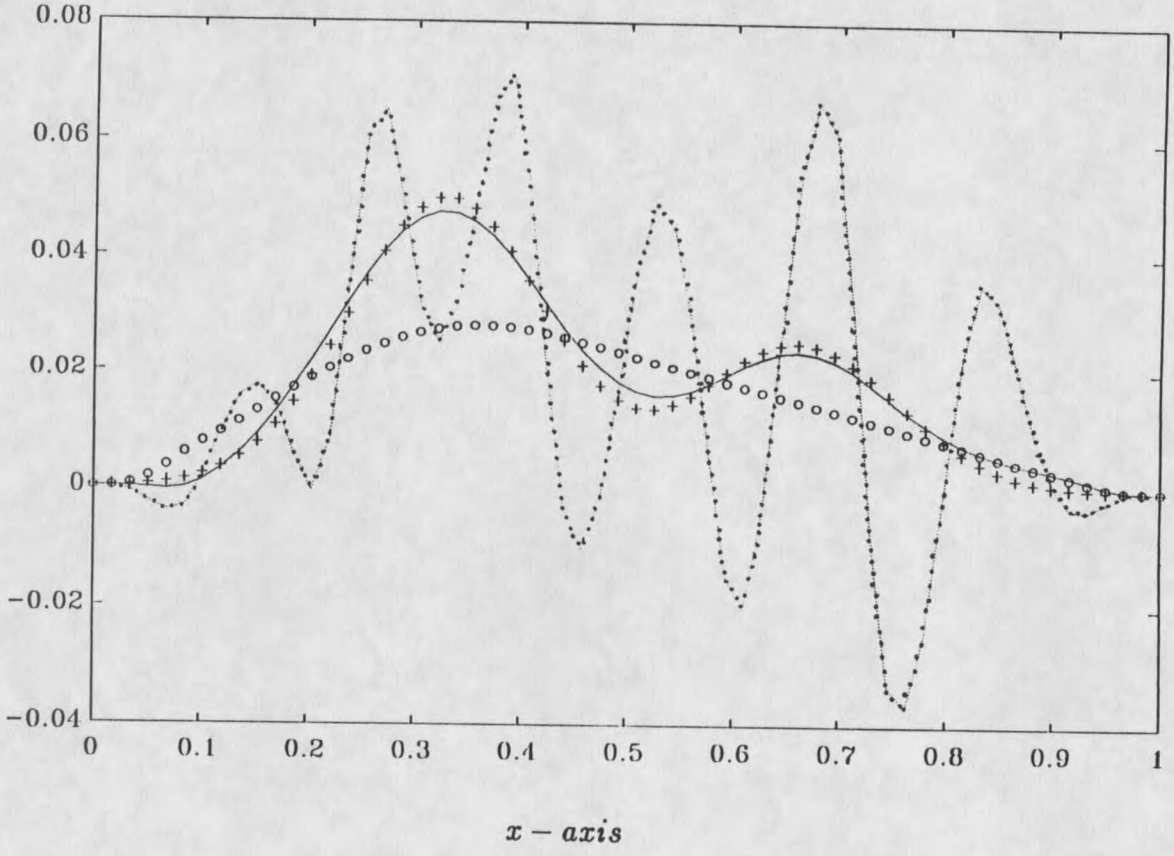


Figure 7. Approximate Solutions for $h = 0.2$.

Figure 8 shows the norm of the true error $\|e_\alpha\| = \|f_\alpha - f\|$ (indicated by o's) and the GCV functional (indicated by stars) as functions of α. The true error increases sharply as α becomes very small. On the other hand, the GCV stays very flat.

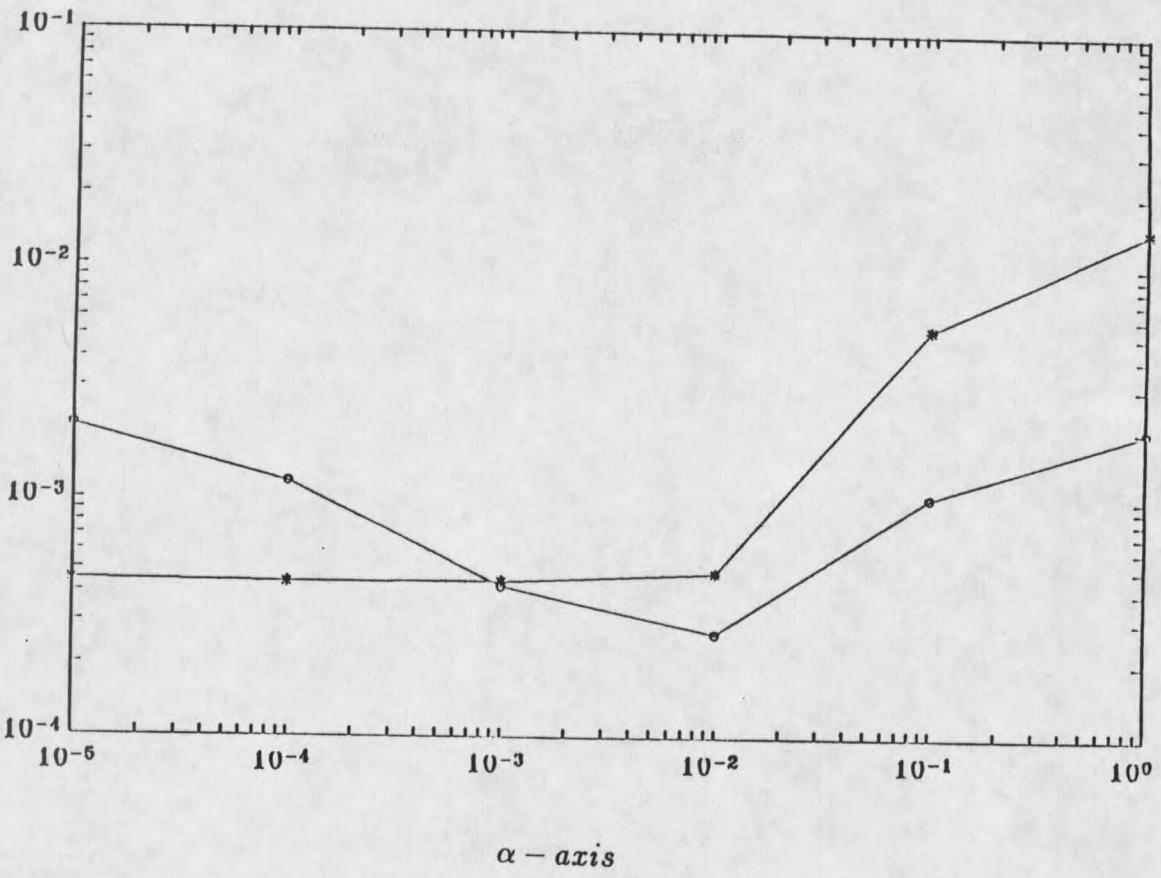


Figure 8. $\|e(\alpha)\|$ and $V(\alpha)$ vs α (1-D case).

In the 2-D case the true magnetic relief function was taken to be

$$f(x,y) = a_1\ exp(-d_1(x-x_1)^2 - e_1(y-y_1)^2) +$$

$$a_2\ exp(-d_2(x-x_2)^2 - e_2(y-y_2)^2),$$

with parameters $a_1 = 0.05$, $a_2 = 0.03$, $d_1 = d_2 = e_1 = e_2 = 60$,$x_1 = y_1 = 0.4$, $x_2 = y_2 = 0.6$. The error was chosen as in the 1-D case. We took basis functions to be tensor products of cubic splines. A total of $100 = 10^2$ basis functions and

$225 = 15^2$ data points were used. The results for the depth $h = 0.2$, the decreasing values of the regularization parameter $\alpha = 10^{-p}, p = 0, 1, ..., 4$ and true solution are shown in Figure 9. As in the 1-D case too small values of the regularization parameter α cause the numerical solution to oscillate.

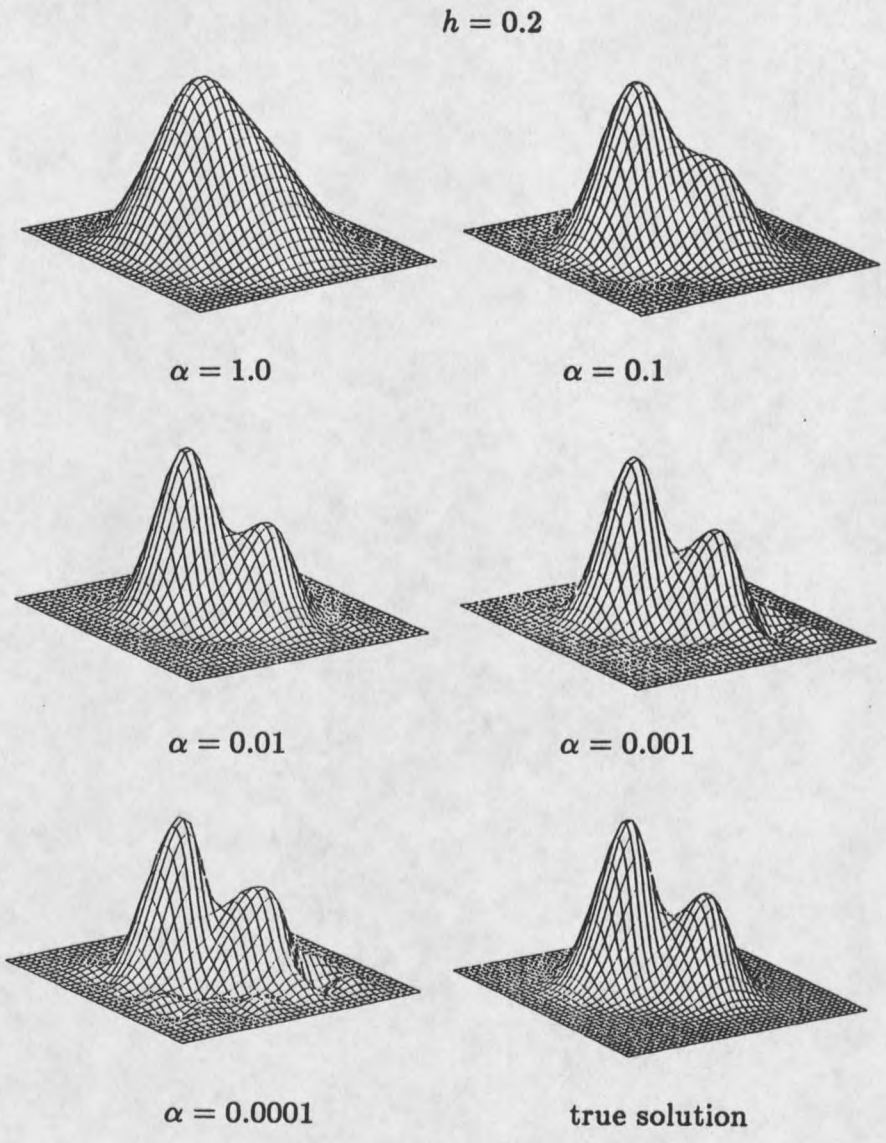


Figure 9. Approximate Solutions.

The solutions on the diagonal $x = y$ are shown in Figure 10. The +'s represent the true solution, the dotted curve corresponds to the regularized solution with $\alpha = 10^{-4}$, and the solid line represents the regularized numerical solution, which is the best in the sense of the H^1 norm.

Figure 11 shows the norm of the true error $\|e_\alpha\| = \|f_\alpha - f\|$ (indicated by o's) and the GCV functional $V(\alpha)$ (indicated by stars) as functions of α. Note that the true error at first decreases with decreasing α, but then increases noticeably as α becomes small. $V(\alpha)$ follows this behavior somewhat, but it stays flat for small α and has no well-defined minimizer.

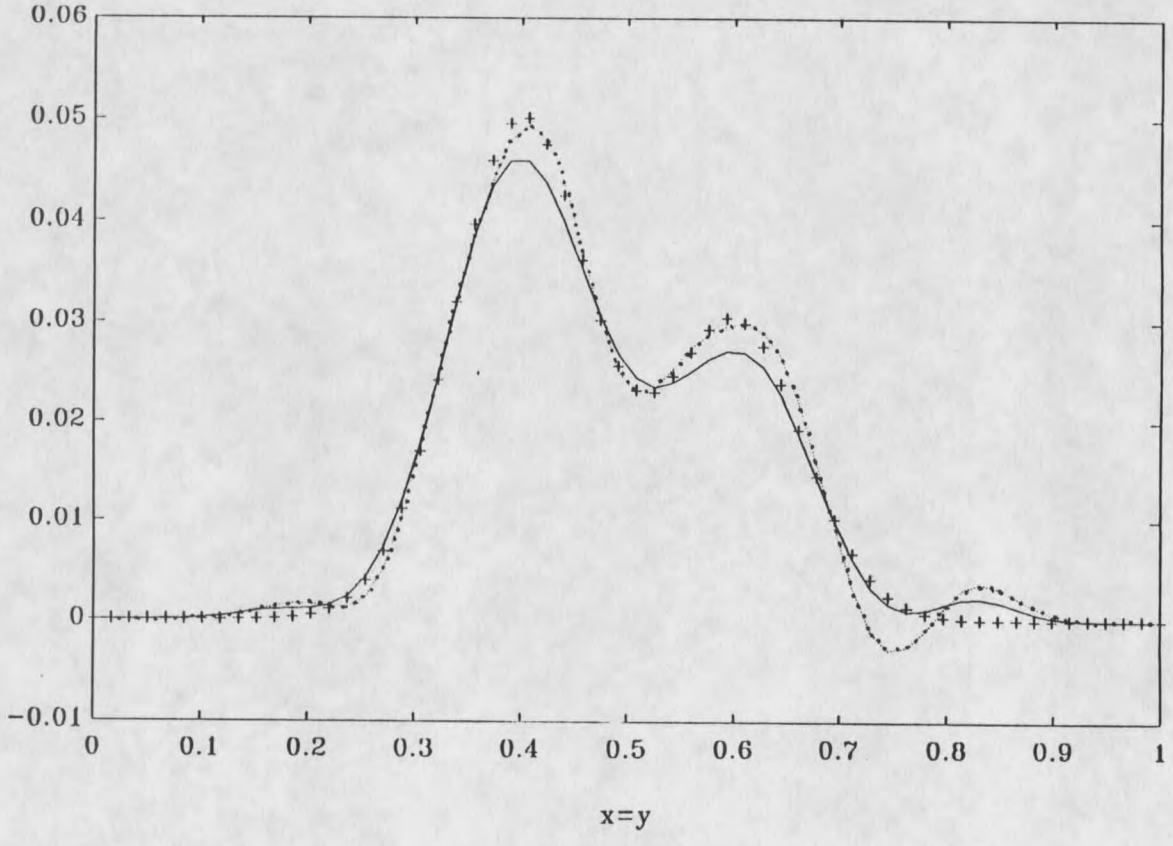


Figure 10. Approximate Solutions on Diagonal $x = y$.

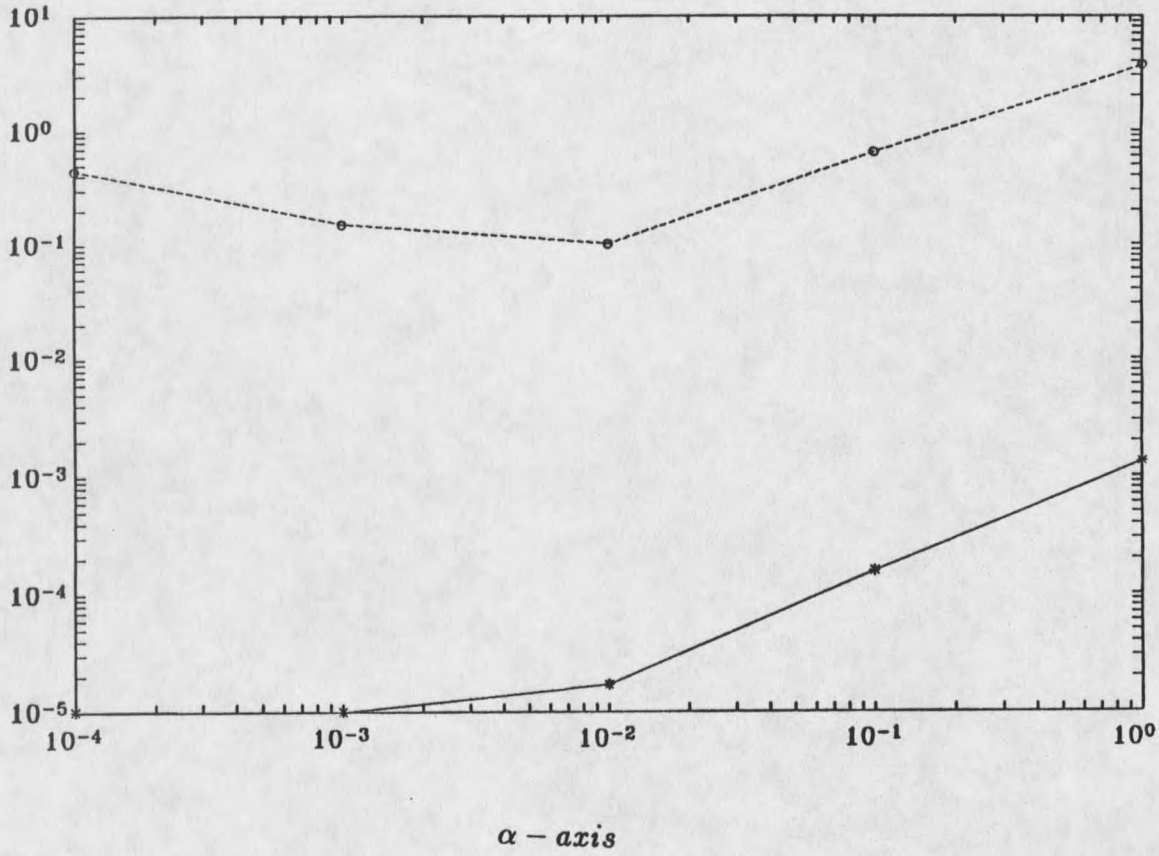


Figure 11. $\|e(\alpha)\|$ and $V(\alpha)$ vs α (2-D case).

REFERENCES CITED

1. Koch, I. and Tarlowski, C. "The Magnetic Relief Problem", *The 1986 Workshop on Inverse Problems.*, R.S. Anderssen and G.N. Newsam, Eds., Centre for Mathematical Analysis, Australian National University, Canberra ACT 2601.

2. Kristensson, G. and Vogel, C.R. "Inverse Problems for Acoustic Waves Using the Penalised Likelihood Method", *Inverse Problems* 2 (1986) pp. 461-479.

3. Tikhonov, A.N. and Arsenin, V.N. *Solutions of Ill-Posed Problems*, John Wiley, New York, 1977.

4. Morozov, V.A *Methods for Solving Incorrectly Posed Problems*, Springer Verlag, New York, 1984.

5. Groetsch, C.W. *The Theory of Tikhonov Regularization for Fredholm Equations of the First Kind*, Pitman Boston, 1984.

6. Vogel, C.R. "Optimal Choice of a Truncation Level for the Truncated SVD Solution of Linear First Kind Integral Equations when Data are Noisy", *SIAM J. Numer. Anal.* 23 (1986) pp. 109-117.

7. Baker, L., Fox, D.F., Meyer, D.F. and Wright, K. "Numerical Solution of Fredholm Integral Equations of the First Kind", *Comput. J.* 7 (1964) pp. 141-148.

8. Hanson, R.J. "A Numerical Method for Fredholm Integral Equations of the First Kind Using Singular Values", *SIAM J. Numer. Anal.* 8 (1971) pp. 616-622.

9. Lee, J.W. and Prenter, P.M. "An Analysis of the Numerical Solution of Fredholm Integral Equations of the First Kind", *Numer. Math.* 30 (1978) pp. 1-23.

10. Fridman, V. "Method of Successive Approximations for Fredholm Integral Equations of the First Kind", *Uspehi Mat. Nauk* 11 (1956) pp. 233-234.

11. Landweber, L. "An Iteration Formula for Fredholm Integral Equations of the First Kind", *Amer. J. Math.* 73 (1951) pp. 615-624.

12. O'Sullivan, F. and Wahba, G. "A Cross Validated Bayesian Retrieval Algorithm for Nonlinear Remote Sensing Experiments", *J. Comput. Phys.* 59 (1985) pp. 441- 455.

13. Wahba, G. "Practical Approximate Solutions to Linear Operator Equations when the Data are Noisy", *SIAM J. Numer. Anal.* 14 (1977) pp. 651-667.

14. Locker, J. and Prenter, P.M. "Regularization with Differential Operators. I. General Theory", *J. Math. Anal. and Appl.* 74 (1980) pp. 504-529.

15. Dennis, J.E. and Schnabel, R.B. *Numerical Methods for Unconstrained Optimization and Nonlinear Equations*, Prentice Hall, New Jersey, 1983.

16. Kreyszig, E. *Introductory Functional Analysis with Applications*, Wiley, New York, 1978.

17. Groetsch, C.W. *Elements of Applicable Functional Analysis*, Dekker, New York, 1980.

18. Yosida, K. *Functional Analysis*, Springer Verlag, New York, 1971.

19. Dieudonne, J.A. *Foundations of Modern Analysis*, Academic Press, New York, 1969.

20. Bowman, J.D. and Aladjem, F. "Method for the Determination of Heterogeneity of Antibodies", *J. Theoret. Biol.* 4 (1963) pp. 242-259.

21. Glasko, V.B., Gushchin, G.V. and Starostenko, V.I. "Tikhonov Regularization Applied to the Solution of Nonlinear Systems of Equations", *USSR Comp. Math. Phys.* 16 (1973) pp. 1-10.

22. Cullum, J. "Numerical Differentiation and Regularization", *SIAM J. Numer. Anal.* 8 (1971) pp. 254-265.

23. Gordonova, V.I. and Morozov, V.A. "Numerical Parameter Selection Algorithms in the Regularization Method", *Z. Vycisl. Mat. i Mat. Fiz.* 13 (1973) pp. 539-545.

24. Strand, O.N. and Westwater, E.R. "Statistical Estimation of the Numerical Solution of a Fredholm Equation of the First Kind", *J. Assoc. Comp. Mach.* 15 (1968) pp. 100-114.

25. Adams, R.A. *Sobolev Spaces*, Academic Press, New York, 1975.

26. Axelsson, O. and Barker, V.A. *Finite Element Solution of Boundary Value Problems*, Academic Press, New York, 1984.

27. Taylor, A.E. and Lay, D.C. *Introduction to Functional Analysis*, second edition, Wiley, New York, 1980.

28. Halmos, P.R. *A Hilbert Space Problem Book*, Van Nostrand, New Jersey, 1967.

29. O'Sullivan, F. "A Statistical Perspective on Ill-Posed Linear Problems", *Statistical Science* 1 (1986) pp. 502-527.

30. De Boor, C. *A Practical Guide to Splines*, Springer Verlag, New York, 1978.

31. Gill, P.E., Murray, W. and Wright, M.H. *Practical Optimization*, Academic Press, New York, 1981.

MONTANA STATE UNIVERSITY LIBRARIES
3 1762 10047794 0

AMERICAN BINDERY
TOPEKA KANSAS
2